

## ON THE GEOMETRY OF STABILIZER STATES

HÉCTOR J. GARCÍA,<sup>1</sup> IGOR L. MARKOV,<sup>1</sup> ANDREW W. CROSS<sup>2</sup>

<sup>1</sup> *University of Michigan, EECS, Ann Arbor, MI 48109-2121*  
 {hjgarcia, imarkov}@eecs.umich.edu

<sup>2</sup> *IBM T. J. Watson Research Center*  
 Yorktown Heights, NY 10598

Large-scale quantum computation is likely to require massive quantum error correction (QEC). QEC codes and circuits are described via the stabilizer formalism, which represents *stabilizer states* by keeping track of the operators that preserve them. Such states are obtained by *stabilizer circuits* (consisting of CNOT, Hadamard and Phase gates) and can be represented compactly on conventional computers using  $\Theta(n^2)$  bits, where  $n$  is the number of qubits [17]. As an additional application, the work in [1, 2] suggests the use of superpositions of stabilizer states to represent arbitrary quantum states. To aid in such applications and improve our understanding of stabilizer states, we characterize and count nearest-neighbor stabilizer states, quantify the distribution of angles between pairs of stabilizer states, study succinct stabilizer superpositions and stabilizer bivectors, explore the approximation of non-stabilizer states by single stabilizer states and short linear combinations of stabilizer states, develop an improved inner-product computation for stabilizer states via synthesis of compact canonical stabilizer circuits, propose an orthogonalization procedure for stabilizer states, and evaluate several of these algorithms empirically.

*Keywords:* quantum circuits, computational geometry, inner product, wedge product, exterior product, stabilizer states, stabilizer circuits

*Communicated by:* to be filled by the Editorial

### 1 Introduction

Gottesman [16] and Knill showed that for certain types of quantum circuits known as *stabilizer circuits*, efficient simulation on classical computers is possible. Stabilizer circuits are exclusively composed of *stabilizer gates* — Controlled-NOT, Hadamard and Phase gates (Figure 2a) — followed by measurements in the computational basis. Such circuits are applied to a computational basis state (usually  $|00\dots 0\rangle$ ) and produce output states called *stabilizer states*. The case of unitary stabilizer circuits (without measurement gates) is considered often, e.g., by consolidating measurements at the end [23]. Stabilizer circuits can be simulated in poly-time by keeping track of a set Pauli operators that stabilize<sup>a</sup> the quantum state. Such *stabilizer operators* uniquely represent a stabilizer state up to an unobservable global phase. Equation 1 shows that the number of  $n$ -qubit stabilizer states grows as  $2^{n^2/2}$ , therefore, describing a generic stabilizer state requires at least  $n^2/2$  bits. Despite their compact representation, stabilizer states can exhibit multi-qubit entanglement and are encountered in many quantum information applications such as Bell states, GHZ states, error-correcting codes and one-way quantum computation. To better understand the role stabilizer states play in such applications, researchers have designed techniques to quantify the amount of entan-

<sup>a</sup>An operator  $U$  is said to stabilize a state iff  $U|\psi\rangle = |\psi\rangle$ .

gument [15, 21, 37] in such states and studied related topics such as purification schemes [13], Bell inequalities [18] and equivalence classes [33]. In particular, the authors of [11, 24, 26] show that the uniform distribution over the  $n$ -qubit stabilizer states is an exact 2-design<sup>b</sup>. Therefore, similar to general random quantum states, stabilizer states exhibit a distribution that is close to uniform. Furthermore, the results from [7, 31] show that the entanglement of stabilizer states is nearly maximal and similar to that of general random states. This suggests the possibility of using stabilizer states as proxies for generic quantum states, e.g., represent arbitrary states by superpositions of stabilizer states. To this end, the work in [1] proposes a hierarchy for quantum states based on their complexity — the number of classical bits required to describe the state. Such a hierarchy can be used to describe which classes of states admit polynomial-size classical descriptions of various kinds. To explore the boundaries between these classes, one can design new stabilizer-based representations (e.g., superpositions of stabilizer states and tensor products of such superpositions) that (i) admit polynomial-size descriptions of practical non-stabilizer states, and (ii) facilitate efficient simulation of generic quantum circuits. Our work advances the understanding of the geometry of stabilizer states and develops efficient computation of distances, angles and volumes between them. This line of research can help identify efficient techniques for representing and manipulating new classes of quantum states, rule out inefficient techniques, and quantify entanglement of relevant states. Our work contributes the following:

- (1) We quantify the distribution of angles between pairs of stabilizer states and characterize *nearest-neighbor stabilizer states*.
- (2) We study linearly-dependent sets of stabilizer states and show that every linearly-dependent triplet of such states that are non-parallel to each other includes two pairs of nearest neighbors and one pair of orthogonal states. Such triplets are illustrated in Figure 1. We also describe an orthogonalization procedure for stabilizer states that exploits this rather uniform nearest-neighbor structure.
- (3) We show that: (i) for any  $n$ -qubit stabilizer state  $|\psi\rangle$ , there are at least  $5(2^n - 1)$  states  $|\varphi\rangle$  such that  $|\psi \wedge \varphi\rangle$  is a *stabilizer bivector*, and (ii) the norm of the wedge product between any two stabilizer states is  $\sqrt{1 - 2^{-k}}$ , where  $0 \leq k \leq n$ .

<sup>b</sup> A state  $k$ -design is an ensemble of states such that, when one state is chosen from the ensemble and copied  $k$  times, it is indistinguishable from a uniformly random state [19, 11].

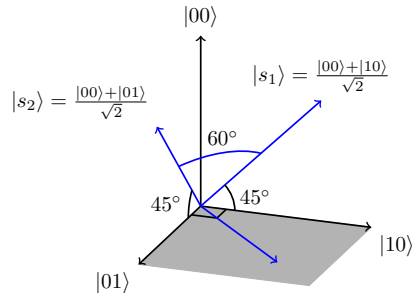


Fig. 1. The angle between any stabilizer state and its nearest neighbors is  $45^\circ$  and the distance is  $\sqrt{2} - \sqrt{2}$ . Here,  $|s_1\rangle$  is a nearest neighbor of both  $|00\rangle$  and  $|10\rangle$ . Similarly,  $|s_2\rangle$  is a nearest neighbor of  $|00\rangle$  and  $|01\rangle$ . The angle between these two nearest neighbors of  $|00\rangle$  is  $60^\circ$ . Consider the linearly-dependent triplets  $\{|00\rangle, |10\rangle, |s_1\rangle\}$  and  $\{|00\rangle, |01\rangle, |s_2\rangle\}$ . Each set contains two pairs of nearest neighbors and one pair of orthogonal states.

- (4) We explore the approximation of non-stabilizer states by single stabilizer states and short superpositions of stabilizer states.
- (5) We exploit our analysis of the geometry of stabilizer states to design algorithms for the following fundamental tasks: (i) synthesizing new *canonical stabilizer circuits* that reduce the number of gates required for QECC encoding procedures, (ii) computing the inner product between stabilizer states, and (iii) computing stabilizer bivectors.

**Geometric properties of stabilizer states.** We define *nearest neighbor* of an  $n$ -qubit stabilizer state  $|\psi\rangle$  as a state  $|\phi\rangle$  such that  $|\langle\psi|\phi\rangle| = 1/\sqrt{2}$ , the largest possible value  $\neq 1$  (Corollary 3). In Theorem 13, we prove that every stabilizer state has exactly  $4(2^n - 1)$  nearest neighbors. Theorem 15 generalizes this result to the case of  $k$ -neighbors, where  $0 < k \leq n$ . We use these results to quantify the distribution of angles between any one stabilizer state and all other stabilizer states. We show that, for sufficiently large  $n$ ,  $1/3$  of all stabilizer states are orthogonal to  $|\psi\rangle$  (Corollary 6) and the fraction of  $k$ -neighbors tends to zero for  $0 < k < n - 4$  (Theorem 16). Therefore,  $2/3$  of all stabilizer states are oblique to  $|\psi\rangle$  and this fraction is dominated by the  $k$ -neighbors, where  $n - 4 \leq k \leq n$ . These findings suggest a rather uniform geometric structure for stabilizer states. This is further evidenced by two additional facts. First, for any  $n$ -qubit stabilizer state  $|\psi\rangle$ , there exists a set of  $2^n - 1$  nearest neighbors to  $|\psi\rangle$  that lie at  $60^\circ$  angles to each other (Corollary 5). Second, every linearly-dependent triplet of stabilizer states that are non-parallel to each other includes two pairs of nearest neighbors and one pair of orthogonal states (Corollary 7). Additionally, Theorem 19 shows that there are  $5(2^n - 1)$  states  $|\varphi\rangle$  (including all nearest-neighbor states) such that the wedge product  $|\phi\rangle = |\psi \wedge \varphi\rangle$  can also be represented compactly (up to a phase) using the stabilizer formalism. We call such a state a *stabilizer bivector*. In Proposition 20, we prove that the norm of any stabilizer bivector and thus the area of the parallelogram formed by any two stabilizer states is  $\sqrt{1 - 2^{-k}}$  for  $0 \leq k \leq n$ .

**Embedding of stabilizer geometry in the Hilbert space.** In Section 4, we describe how the discrete embedding of stabilizer geometry in Hilbert space complicates several natural geometric tasks. Our results on the geometric properties of stabilizer states imply that there are significantly more stabilizer states than the dimension of the Hilbert space in which they are embedded (Theorem 17), and that they are arranged in a fairly uniform pattern (Corollaries 5 and 7). These factors suggest that, if one seeks a stabilizer state closest to a given arbitrary quantum state, local search appears a promising candidate. To the contrary, we show that local search *does not* guarantee finding such stabilizer states (Section 4.1). The second natural task we consider is representing or approximating a given arbitrary quantum state by a short linear combination of stabilizer states. Again, having considerably more stabilizer states than the dimension of the Hilbert space may suggest a positive result at first. However, we demonstrate a family of quantum states that exhibits *asymptotic orthogonality* to all stabilizer states and can thus be neither represented nor approximated by short superpositions of stabilizer states (Theorem 22). Furthermore, we show in Proposition 23 that the maximal radius of any  $2^n$ -dimensional ball centered at a point on the unit sphere that does not contain any  $n$ -qubit stabilizer states cannot exceed  $\sqrt{2}$ , but approaches  $\sqrt{2}$  as  $n \rightarrow \infty$ .

**Computational geometry of stabilizer states.** Angles between stabilizer states were

$$H = \frac{1}{\sqrt{2}} \begin{pmatrix} 1 & 1 \\ 1 & -1 \end{pmatrix} \quad P = \begin{pmatrix} 1 & 0 \\ 0 & i \end{pmatrix}$$

$$CNOT = \begin{pmatrix} 1 & 0 & 0 & 0 \\ 0 & 1 & 0 & 0 \\ 0 & 0 & 0 & 1 \\ 0 & 0 & 1 & 0 \end{pmatrix}$$

Fig. 2. (a) Stabilizer gates Hadamard (H), Phase (P) and Controlled-NOT (CNOT).

$$X = \begin{pmatrix} 0 & 1 \\ 1 & 0 \end{pmatrix} \quad Y = \begin{pmatrix} 0 & -i \\ i & 0 \end{pmatrix}$$

$$Z = \begin{pmatrix} 1 & 0 \\ 0 & -1 \end{pmatrix}$$

Fig. 1. (b) The Pauli matrices.

discussed in [2], where the authors describe possible values for such angles and outline an inner-product computation that involves the synthesis of a *basis-normalization stabilizer circuit* that maps a stabilizer state to a computational basis state. We observe that this circuit-synthesis procedure is the computational bottleneck of the algorithm and thus any improvements to this synthesis process translate into increased performance of the overall algorithm. It was also shown in [2] that, for any unitary stabilizer circuit, there exists an equivalent block-structured *canonical circuit* that applies a block of Hadamard ( $H$ ) gates only, followed by a block of CNOT ( $C$ ) only, then a block of Phase ( $P$ ) gates only, and so on in the 7-block sequence  $H-C-P-C-P-C-H$ . The number of gates in any  $H$  and  $P$  block is at most  $2n$  and  $4n$ , respectively, so the total number of gates for such canonical circuits is dominated by the  $C$  blocks, which contain  $O(n^2/\log n)$  gates [29]. Therefore, reducing the number of  $C$  blocks (or those involving other controlled operations) leads to more compact circuits that minimize the build-up of decoherence when implementing QECC encoding procedures. Using an alternative representation for stabilizer states, the work in [32] proves the existence of canonical circuits with the shorter sequence  $H-C-X-P-CZ$ , where the  $X$  and  $CZ$  blocks consist of NOT and Controlled-Z (CPHASE) gates, respectively. Such circuits contain only two controlled-op blocks (as compared to three  $C$  blocks in the 7-block sequence from [2]) but no algorithms are available in literature to synthesize these circuits for an arbitrary stabilizer state. We describe an algorithm for synthesizing canonical circuits with the block sequence  $H-C-CZ-P-H$ . Our circuits are therefore close to the smallest known circuits proposed in [32]. Our canonical circuits improve the computation of inner products, helping us outperform the inner-product algorithm based on non-canonical circuits proposed in [4]. Furthermore, we leverage our circuit-synthesis technique and inner-product algorithm to compute stabilizer bivectors efficiently.

For comparison, we implemented the circuit-synthesis portion of the algorithm from [4]. Our algorithm produces circuits with less than half as many gates on average and runs roughly  $2\times$  faster. Furthermore, our synthesis approach produces canonical circuits given any input stabilizer state by first obtaining a *canonical generator set* for the state. We describe a separate algorithm for reducing an arbitrary stabilizer generator set to its canonical form.

This paper is structured as follows. Section 2 reviews the stabilizer formalism and relevant algorithms for manipulating stabilizer-based representations of quantum states. Our findings related to geometric structure of stabilizer states are described in Sections 3 and 4. Section 5 describes our algorithms for circuit synthesis, inner product computation and construction of stabilizer bivectors. In Section 6, we evaluate the performance of our inner-product algorithm, and Section 7 closes with concluding remarks.

## 2 Background and Previous Results

Gottesman [17] developed a description for quantum states involving the *Heisenberg representation* often used by physicists to describe atomic phenomena. In this model, quantum states are described by keeping track of their symmetries rather than explicitly maintaining the amplitudes of exponentially-large vectors. The symmetries are operators for which these states are 1-eigenvectors. Algebraically, symmetries form *group* structures, which can be specified compactly by group generators. This approach, also known as the *stabilizer formalism*, facilitates particularly efficient manipulation of an important class of quantum states.

### 2.1 The stabilizer formalism

A unitary operator  $U$  *stabilizes* a state  $|\psi\rangle$  if  $|\psi\rangle$  is a 1-eigenvector of  $U$ , i.e.,  $U|\psi\rangle = |\psi\rangle$  [16, 28]. We are interested in operators  $U$  derived from the Pauli matrices shown in Figure 2b. The following table lists the one-qubit states stabilized by the Pauli matrices.

$$\begin{array}{ll} X : & (|0\rangle + |1\rangle)/\sqrt{2} \\ Y : & (|0\rangle + i|1\rangle)/\sqrt{2} \\ Z : & |0\rangle \end{array} \quad \begin{array}{ll} -X : & (|0\rangle - |1\rangle)/\sqrt{2} \\ -Y : & (|0\rangle - i|1\rangle)/\sqrt{2} \\ -Z : & |1\rangle \end{array}$$

Observe that  $I$  stabilizes all states and  $-I$  does not stabilize any state. As an example, the entangled state  $(|00\rangle + |11\rangle)/\sqrt{2}$  is stabilized by the Pauli operators  $X \otimes X$ ,  $-Y \otimes Y$ ,  $Z \otimes Z$  and  $I \otimes I$ . As shown in Table 1, it turns out that the Pauli matrices along with  $I$  and the multiplicative factors  $\pm 1$ ,  $\pm i$ , form a *closed group* under matrix multiplication [28]. Formally, the *Pauli group*  $\mathcal{G}_n$  on  $n$  qubits consists of the  $n$ -fold tensor product of Pauli matrices,  $P = i^k P_1 \otimes \cdots \otimes P_n$  such that  $P_j \in \{I, X, Y, Z\}$  and  $k \in \{0, 1, 2, 3\}$ . For brevity, the tensor-product symbol is often omitted so that  $P$  is denoted by a string of  $I$ ,  $X$ ,  $Y$  and  $Z$  characters or *Pauli literals* and a separate integer value  $k$  for the phase  $i^k$ . This string-integer pair representation allows us to compute the product of Pauli operators without explicitly computing the tensor products,<sup>c</sup> e.g.,  $(-IIXI)(iIYII) = -iIYXI$ . Since  $|\mathcal{G}_n| = 4^{n+1}$ ,  $\mathcal{G}_n$  can have at most  $\log_2 |\mathcal{G}_n| = \log_2 4^{n+1} = 2(n+1)$  irredundant generators [28]. The key idea behind the stabilizer formalism is to represent an  $n$ -qubit quantum state  $|\psi\rangle$  by its *stabilizer group*  $S(|\psi\rangle)$  — the subgroup of  $\mathcal{G}_n$  that stabilizes  $|\psi\rangle$ . As the following theorem shows, if  $|S(|\psi\rangle)| = 2^n$ , the group uniquely specifies  $|\psi\rangle$ .

**Theorem 1.** *For an  $n$ -qubit pure state  $|\psi\rangle$ , there exists a  $k \leq n$  such that  $S(|\psi\rangle) \cong \mathbb{Z}_2^k$ . If  $k = n$ ,  $|\psi\rangle$  is specified uniquely by  $S(|\psi\rangle)$  and is called a stabilizer state.*

**Proof.** (i) To prove that  $S(|\psi\rangle)$  is commutative, let  $P, Q \in S(|\psi\rangle)$  such that  $PQ|\psi\rangle = |\psi\rangle$ . If  $P$  and  $Q$  anticommute,  $-QP|\psi\rangle = -Q(P|\psi\rangle) = -Q|\psi\rangle = -|\psi\rangle \neq |\psi\rangle$ . Thus,  $P$  and  $Q$  cannot both be elements of  $S(|\psi\rangle)$ .

<sup>c</sup>This holds true due to the identity:  $(A \otimes B)(C \otimes D) = (AC \otimes BD)$ .

Table 1. Multiplication table for Pauli matrices. Shaded cells indicate anticommuting products.

	$I$	$X$	$Y$	$Z$
$I$	$I$	$X$	$Y$	$Z$
$X$	$X$	$I$	$iZ$	$-iY$
$Y$	$Y$	$-iZ$	$I$	$iX$
$Z$	$Z$	$iY$	$-iX$	$I$

(ii) To prove that every element of  $S(|\psi\rangle)$  is of degree 2, let  $P \in S(|\psi\rangle)$  such that  $P|\psi\rangle = |\psi\rangle$ . Observe that  $P^2 = i^l I$  for  $l \in \{0, 1, 2, 3\}$ . Since  $P^2|\psi\rangle = P(P|\psi\rangle) = P|\psi\rangle = |\psi\rangle$ , we obtain  $i^l = 1$  and  $P^2 = I$ .

(iii) From group theory, a finite Abelian group with  $a^2 = a$  for every element must be  $\cong \mathbb{Z}_2^k$ .

(iv) We now prove that  $k \leq n$ . First note that each independent generator  $P \in S(|\psi\rangle)$  imposes the linear constraint  $P|\psi\rangle = |\psi\rangle$  on the  $2^n$ -dimensional vector space. The subspace of vectors that satisfy such a constraint has dimension  $2^{n-1}$ , or half the space. Let  $\text{gen}(|\psi\rangle)$  be the set of generators for  $S(|\psi\rangle)$ . We add independent generators to  $\text{gen}(|\psi\rangle)$  one by one and impose their linear constraints, to limit  $|\psi\rangle$  to the shared 1-eigenvector. Thus the size of  $\text{gen}(|\psi\rangle)$  is at most  $n$ . In the case  $|\text{gen}(|\psi\rangle)| = n$ , the  $n$  independent generators reduce the subspace of possible states to dimension one. Thus,  $|\psi\rangle$  is uniquely specified.  $\square$

The proof of Theorem 1 shows that  $S(|\psi\rangle)$  is specified by only  $\log_2 2^n = n$  *irredundant stabilizer generators*. Therefore, an arbitrary  $n$ -qubit stabilizer state can be represented by a *stabilizer matrix*  $\mathcal{M}$  whose rows represent a set of generators  $g_1, \dots, g_n$  for  $S(|\psi\rangle)$ . (Hence we use the terms *generator set* and *stabilizer matrix* interchangeably.) Since each  $g_i$  is a string of  $n$  Pauli literals, the size of the matrix is  $n \times n$ . The phases of each  $g_i$  are stored separately using a vector of  $n$  integers. Therefore, the storage cost for  $\mathcal{M}$  is  $\Theta(n^2)$ , which is an *exponential improvement* over the  $O(2^n)$  cost often encountered in vector-based representations.

Theorem 1 suggests that Pauli literals can be represented using only two bits, e.g.,  $00 = I$ ,  $01 = Z$ ,  $10 = X$  and  $11 = Y$ . Therefore, a stabilizer matrix can be encoded using an  $n \times 2n$  binary matrix or *tableau*. The advantage of this approach is that this literal-to-bits mapping induces an isomorphism  $\mathbb{Z}_2^{2n} \rightarrow \mathcal{G}_n$  because vector addition in  $\mathbb{Z}_2^{2n}$  is equivalent to multiplication of Pauli operators up to a global phase. The tableau implementation of the stabilizer formalism is covered in [2, 28].

**Proposition 2.** *The number of  $n$ -qubit pure stabilizer states is given by*

$$\mathcal{N}(n) = 2^n \prod_{k=0}^{n-1} (2^{n-k} + 1) = 2^{(.5+o(1))n^2} \quad (1)$$

The proof of Proposition 2 can be found in [2]. An alternate interpretation of Equation 1 is given by the simple recurrence relation  $\mathcal{N}(n) = 2(2^n + 1)\mathcal{N}(n-1)$  with base case  $\mathcal{N}(1) = 6$ . For example, for  $n = 2$  the number of stabilizer states is 60, and for  $n = 3$  it is 1080. This recurrence relation stems from the fact that there are  $2^n + 1$  ways of combining the generators of the  $\mathcal{N}(n-1)$  states with additional Pauli matrices to form valid  $n$ -qubit generators. The factor of 2 accounts for the increase in the number of possible sign configurations. Table 2 and Appendix A list all two-qubit and three-qubit stabilizer states, respectively.

**Proposition 3.** *The tensor product  $|\psi\rangle \otimes |\varphi\rangle$  of two stabilizer states is a stabilizer state.*

**Proof.** Consider two Pauli operators,  $P$  and  $Q$ , which stabilize the  $n$ -qubit state  $|\psi\rangle$  and the  $m$ -qubit state  $|\varphi\rangle$ , respectively. The  $(n+m)$ -qubit state  $|\psi\rangle \otimes |\varphi\rangle$  is stabilized by  $P \otimes Q = PQ$  since  $PQ|\psi\rangle|\varphi\rangle = P|\psi\rangle Q|\varphi\rangle = |\psi\rangle|\varphi\rangle$ . Let  $\{P_1, \dots, P_n\}$  and  $\{Q_1, \dots, Q_m\}$  be sets of generators for  $S(|\psi\rangle)$  and  $S(|\varphi\rangle)$ , respectively. We create an  $(n+m)$ -element set of Pauli operators as follows,  $P_j \otimes I^{\otimes m}$ ,  $j \in \{1, \dots, n\}$  and  $I^{\otimes n} \otimes Q_k$ ,  $k \in \{1, \dots, m\}$ . This is a generator set for  $S(|\psi\rangle|\varphi\rangle)$  because each of the operators in the set stabilizes  $|\psi\rangle|\varphi\rangle$  and the set generates all tensor products  $P_j Q_k$ .  $\square$

Table 2. Sixty two-qubit stabilizer states and their corresponding Pauli generators. Shorthand notation represents a stabilizer state as  $\alpha_0, \alpha_1, \alpha_2, \alpha_3$  where  $\alpha_i$  are the normalized amplitudes of the basis states. The basis states are emphasized in bold. The first column lists states whose generators do not include an upfront minus sign, and other columns introduce the signs. A sign change creates an orthogonal vector. Therefore, each row of the table gives an orthogonal basis. The cells in dark grey indicate stabilizer states with four non-zero basis amplitudes, i.e.,  $\alpha_i \neq 0 \forall i$ . The  $\angle$  column indicates the angle between that state and  $|00\rangle$ , which has twelve nearest-neighbor states (light gray) and 15 orthogonal states ( $\perp$ ).

	STATE	GEN'TORS	$\angle$	STATE	GEN'TORS	$\angle$	STATE	GEN'TORS	$\angle$	STATE	GEN'TORS	$\angle$
SEPARABLE	<b>1, 1, 1, 1</b>	IX, XI	$\pi/3$	<b>1, -1, 1, -1</b>	-IX, XI	$\pi/3$	<b>1, 1, -1, -1</b>	IX, -XI	$\pi/3$	<b>1, -1, -1, 1</b>	-IX, -XI	$\pi/3$
	<b>1, 1, <math>i</math>, <math>i</math></b>	IX, YI	$\pi/3$	<b>1, -1, <math>i</math>, <math>-i</math></b>	-IX, YI	$\pi/3$	<b>1, 1, <math>-i</math>, <math>-i</math></b>	IX, -YI	$\pi/3$	<b>1, -1, <math>-i</math>, <math>i</math></b>	-IX, -YI	$\pi/3$
	<b>1, 1, 0, 0</b>	IX, ZI	$\pi/4$	<b>1, -1, 0, 0</b>	-IX, ZI	$\pi/4$	<b>0, 0, 1, 1</b>	IX, -ZI	$\perp$	<b>0, 0, 1, -1</b>	-IX, -ZI	$\perp$
	<b>1, <math>i</math>, 1, <math>i</math></b>	IY, XI	$\pi/3$	<b>1, -<math>i</math>, 1, <math>-i</math></b>	-IY, XI	$\pi/3$	<b>1, <math>i</math>, -1, <math>-i</math></b>	IY, -XI	$\pi/3$	<b>1, -<math>i</math>, -1, <math>i</math></b>	-IY, -XI	$\pi/3$
	<b>1, <math>i</math>, <math>i</math>, -1</b>	IY, YI	$\pi/3$	<b>1, -<math>i</math>, <math>i</math>, 1</b>	-IY, YI	$\pi/3$	<b>1, <math>i</math>, -<math>i</math>, 1</b>	IY, -YI	$\pi/3$	<b>1, -<math>i</math>, -<math>i</math>, -1</b>	-IY, -YI	$\pi/3$
	<b>1, <math>i</math>, 0, 0</b>	IY, ZI	$\pi/4$	<b>1, -<math>i</math>, 0, 0</b>	-IY, ZI	$\pi/4$	<b>0, 0, 1, <math>i</math></b>	IY, -ZI	$\perp$	<b>0, 0, 1, <math>-i</math></b>	-IY, -ZI	$\perp$
	<b>1, 0, 1, 0</b>	IZ, XI	$\pi/4$	<b>0, 1, 0, 1</b>	-IZ, XI	$\perp$	<b>1, 0, -1, 0</b>	IZ, -XI	$\pi/4$	<b>0, 1, 0, -1</b>	-IZ, -XI	$\perp$
	<b>1, 0, <math>i</math>, 0</b>	IZ, YI	$\pi/4$	<b>0, 1, 0, <math>i</math></b>	-IZ, YI	$\perp$	<b>1, 0, -<math>i</math>, 0</b>	IZ, -YI	$\pi/4$	<b>0, 1, 0, <math>-i</math></b>	-IZ, -YI	$\perp$
	<b>1, 0, 0, 0</b>	<b>IZ, ZI</b>	0	<b>0, 1, 0, 0</b>	<b>-IZ, ZI</b>	$\perp$	<b>0, 0, 1, 0</b>	<b>IZ, -ZI</b>	$\perp$	<b>0, 0, 0, 1</b>	<b>-IZ, -ZI</b>	$\perp$
ENTANGLED	<b>0, 1, 1, 0</b>	XX, YY	$\perp$	<b>1, 0, 0, -1</b>	-XX, YY	$\pi/4$	<b>1, 0, 0, 1</b>	XX, -YY	$\pi/4$	<b>0, 1, -1, 0</b>	-XX, -YY	$\perp$
	<b>1, 0, 0, <math>i</math></b>	XY, YX	$\pi/4$	<b>0, 1, <math>i</math>, 0</b>	-XY, YX	$\perp$	<b>0, 1, -<math>i</math>, 0</b>	XY, -YX	$\perp$	<b>1, 0, 0, <math>-i</math></b>	-XY, -YX	$\pi/4$
	<b>1, 1, 1, -1</b>	XZ, ZX	$\pi/3$	<b>1, 1, -1, 1</b>	-XZ, ZX	$\pi/3$	<b>1, -1, 1, 1</b>	XZ, -ZX	$\pi/3$	<b>1, -1, -1, -1</b>	-XZ, -ZX	$\pi/3$
	<b>1, <math>i</math>, 1, <math>-i</math></b>	XZ, ZY	$\pi/3$	<b>1, <math>i</math>, -1, <math>i</math></b>	-XZ, ZY	$\pi/3$	<b>1, -<math>i</math>, 1, <math>i</math></b>	XZ, -ZY	$\pi/3$	<b>1, -<math>i</math>, -1, <math>-i</math></b>	-XZ, -ZY	$\pi/3$
	<b>1, 1, <math>i</math>, <math>-i</math></b>	YZ, ZX	$\pi/3$	<b>1, 1, -<math>i</math>, <math>i</math></b>	-YZ, ZX	$\pi/3$	<b>1, -1, <math>i</math>, <math>i</math></b>	YZ, -ZX	$\pi/3$	<b>1, -1, -<math>i</math>, <math>-i</math></b>	-YZ, -ZX	$\pi/3$
	<b>1, <math>i</math>, <math>i</math>, 1</b>	YZ, ZY	$\pi/3$	<b>1, <math>i</math>, -<math>i</math>, -1</b>	-YZ, ZY	$\pi/3$	<b>1, -<math>i</math>, <math>i</math>, -1</b>	YZ, -ZY	$\pi/3$	<b>1, -<math>i</math>, -<math>i</math>, 1</b>	-YZ, -ZY	$\pi/3$

**Observation 4.** Consider a stabilizer state  $|\psi\rangle$  represented by a set of generators of its stabilizer group  $S(|\psi\rangle)$ . Recall from the proof of Theorem 1 that, since  $S(|\psi\rangle) \cong \mathbb{Z}_2^n$ , each generator imposes a linear constraint on  $|\psi\rangle$ . Therefore, the set of generators can be viewed as a system of linear equations whose solution yields the  $2^k$  (for some  $k$  between 0 and  $n$ ) non-zero computational basis amplitudes that make up  $|\psi\rangle$ . Thus, one needs to perform Gaussian elimination to obtain such basis amplitudes from a generator set.

**Canonical stabilizer matrices.** Although stabilizer states are uniquely determined by their stabilizer group, the set of generators may be selected in different ways. For example, the state  $|\psi\rangle = (|00\rangle + |11\rangle)/\sqrt{2}$  is uniquely specified by any of the following:

$$\mathcal{M}_1 = \begin{vmatrix} XX \\ ZZ \end{vmatrix} \quad \mathcal{M}_2 = \begin{vmatrix} XX \\ -YY \end{vmatrix} \quad \mathcal{M}_3 = \begin{vmatrix} -YY \\ ZZ \end{vmatrix}$$

One obtains  $\mathcal{M}_2$  from  $\mathcal{M}_1$  by left-multiplying the second row by the first. Similarly, one can also obtain  $\mathcal{M}_3$  from  $\mathcal{M}_1$  or  $\mathcal{M}_2$  via row multiplication. Observe that, multiplying any row by itself yields  $II$ , which stabilizes  $|\psi\rangle$ . However,  $II$  cannot be used as a stabilizer generator because it is redundant and carries no information about the structure of  $|\psi\rangle$ . This also holds true in general for  $\mathcal{M}$  of any size. Any stabilizer matrix can be rearranged by applying sequences of elementary row operations in order to obtain a particular matrix structure. Such operations do not modify the stabilizer state. The elementary row operations that can be performed on a stabilizer matrix are transposition, which swaps two rows of the matrix, and multiplication, which left-multiplies one row with another. Such operations allow one to rearrange the stabilizer matrix in a series of steps that resemble Gauss-Jordan elimination.<sup>d</sup> Given an  $n \times n$  stabilizer matrix, row transpositions are performed in constant time<sup>e</sup> while

<sup>d</sup>Since Gaussian elimination essentially inverts the  $n \times 2n$  matrix, this could be sped up to  $O(n^{2.376})$  time by using fast matrix inversion algorithms. However,  $O(n^3)$ -time Gaussian elimination seems more practical.

<sup>e</sup>Storing pointers to rows facilitates  $O(1)$ -time row transpositions — one simply swaps relevant pointers.

row multiplications require  $\Theta(n)$  time. Algorithm 2.1 rearranges a stabilizer matrix into a *row-reduced echelon form* that contains: (i) a *minimum set* of generators with  $X$  and  $Y$  literals appearing at the top, and (ii) generators containing a *minimum set* of  $Z$  literals only appearing at the bottom of the matrix. This particular stabilizer-matrix structure, shown in Figure 3, defines a canonical representation for stabilizer states [12, 17]. Several row-echelon (standard) forms for stabilizer generators along with relevant algorithms to obtain them have been introduced in the literature [4, 17, 28]. However, such standard forms are not always canonical, e.g, the row-echelon form described in [4] does not guarantee a minimum set of  $Z$  literals. Since most of our algorithms manipulate canonical stabilizer matrices, we will describe in detail our Gaussian-elimination procedure for obtaining the canonical structure depicted in Figure 3. The algorithm iteratively determines which row operations to apply based on the Pauli (non- $I$ ) literals contained in the first row and column of an increasingly smaller submatrix of the full stabilizer matrix. Initially, the submatrix considered is the full stabilizer matrix. After the proper row operations are applied, the dimensions of the submatrix decrease by one until the size of the submatrix reaches one. The algorithm performs this process twice, once to position the rows with  $X(Y)$  literals at the top, and then again to position the remaining rows containing  $Z$  literals only at the bottom. Let  $i \in \{1, \dots, n\}$  and  $j \in \{1, \dots, n\}$  be the index of the first row and first column, respectively, of submatrix  $\mathcal{A}$ . The steps to construct the upper-triangular portion of the row-echelon form shown in Figure 3 are as follows.

1. Let  $k$  be a row in  $\mathcal{A}$  whose  $j^{\text{th}}$  literal is  $X(Y)$ . Swap rows  $k$  and  $i$  such that  $k$  is the first row of  $\mathcal{A}$ . Decrease the height of  $\mathcal{A}$  by one (i.e., increase  $i$ ).
2. For each row  $m \in \{0, \dots, n\}, m \neq i$  that has an  $X(Y)$  in column  $j$ , use row multiplication to set the  $j^{\text{th}}$  literal in row  $m$  to  $I$  or  $Z$ .
3. Decrease the width of  $\mathcal{A}$  by one (i.e., increase  $j$ ).

To bring the matrix to its lower-triangular form, one executes the same procedure with the following difference: (i) step 1 looks for rows that have a  $Z$  literal (instead of  $X$  or  $Y$ ) in column  $j$ , and (ii) step 2 looks for rows that have  $Z$  or  $Y$  literals (instead of  $X$  or  $Y$ ) in column  $j$ . Observe that Algorithm 2.1 ensures that the columns in  $\mathcal{M}$  have at most two distinct types of non- $I$  literals. Since Algorithm 2.1 inspects all  $n^2$  entries in the matrix and performs a constant number of row multiplications each time, its runtime is  $O(n^3)$ .

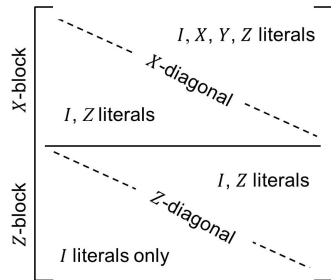


Fig. 3. Canonical (row-reduced echelon) form for stabilizer matrices. The  $X$ -block contains a *minimal* set of rows with  $X/Y$  literals. The rows with  $Z$  literals only appear in the  $Z$ -block. Each block is arranged so that the leading non- $I$  literal of each row is strictly to the right of the leading non- $I$  literal in the row above. The number of Pauli (non- $I$ ) literals in each block is minimal.



**Algorithm 2.1** Canonical form reduction for stabilizer matrices**Input:** Stabilizer matrix  $\mathcal{M}$  for  $S(|\psi\rangle)$  with rows  $R_1, \dots, R_n$ **Output:**  $\mathcal{M}$  is reduced to row-echelon form $\Rightarrow$  ROWSWAP( $\mathcal{M}, i, j$ ) swaps rows  $R_i$  and  $R_j$  of  $\mathcal{M}$  $\Rightarrow$  ROWMULT( $\mathcal{M}, i, j$ ) left-multiplies rows  $R_i$  and  $R_j$ , returns updated  $R_i$ 

```

1:  $i \leftarrow 1$ 
2: for  $j \in \{1, \dots, n\}$  do                                      $\triangleright$  Setup  $X$  block
3:    $k \leftarrow$  index of row  $R_{k \in \{i, \dots, n\}}$  with  $j^{th}$  literal set to  $X(Y)$ 
4:   if  $k$  exists then
5:     ROWSWAP( $\mathcal{M}, i, k$ )
6:     for  $m \in \{0, \dots, n\}$  do
7:       if  $j^{th}$  literal of  $R_m$  is  $X$  or  $Y$  and  $m \neq i$  then
8:          $R_m = \text{ROWMULT}(\mathcal{M}, R_i, R_m)$                         $\triangleright$  Gauss-Jordan elimination step
9:       end if
10:    end for
11:     $i \leftarrow i + 1$ 
12:  end if
13: end for
14: for  $j \in \{1, \dots, n\}$  do                                      $\triangleright$  Setup  $Z$  block
15:    $k \leftarrow$  index of row  $R_{k \in \{i, \dots, n\}}$  with  $j^{th}$  literal set to  $Z$ 
16:   if  $k$  exists then
17:     ROWSWAP( $\mathcal{M}, i, k$ )
18:     for  $m \in \{0, \dots, n\}$  do
19:       if  $j^{th}$  literal of  $R_m$  is  $Z$  or  $Y$  and  $m \neq i$  then
20:          $R_m = \text{ROWMULT}(\mathcal{M}, R_i, R_m)$                         $\triangleright$  Gauss-Jordan elimination step
21:       end if
22:     end for
23:     $i \leftarrow i + 1$ 
24:  end if
25: end for

```

**Definition 1.** Two stabilizer matrices are *similar* if they contain the same Pauli generators with different  $\pm 1$  phases, i.e., the matrices are equivalent up to a phase-vector permutation. Otherwise, the matrices are called *dissimilar*.

**Observation 5.** The number of dissimilar  $n$ -qubit canonical stabilizer matrices is  $\mathcal{N}(n)/2^n$ .

**Stabilizer-circuit simulation.** Observe that the computational-basis states can be characterized as stabilizer states with the following stabilizer-matrix structure.

**Definition 2.** A stabilizer matrix is in its *basis form* if it has the following structure.

$$\begin{array}{c} \pm \\ \pm \\ \vdots \\ \pm \end{array} \begin{bmatrix} Z & I & \cdots & I \\ I & Z & \cdots & I \\ \vdots & \vdots & \ddots & \vdots \\ I & I & \cdots & Z \end{bmatrix}$$

In this matrix form, the  $\pm$  sign of each row along with its corresponding  $Z_j$ -literal designates whether the state of the  $j^{th}$  qubit is  $|0\rangle$  (+) or  $|1\rangle$  (−). Suppose we want to simulate circuit  $\mathcal{C}$ . Stabilizer-based simulation first initializes  $\mathcal{M}$  to specify some basis state  $|\psi\rangle$ . To simulate the action of each gate  $U \in \mathcal{C}$ , we conjugate each row  $g_i$  of  $\mathcal{M}$  by  $U$ .<sup>f</sup> We require that  $Ug_iU^\dagger$  maps to another string of Pauli literals so that the resulting stabilizer matrix

<sup>f</sup>Since  $g_i|\psi\rangle = |\psi\rangle$ , the resulting state  $U|\psi\rangle$  is stabilized by  $Ug_iU^\dagger$  because  $(Ug_iU^\dagger)U|\psi\rangle = Ug_i|\psi\rangle = U|\psi\rangle$ .

Table 3. Transformation of Pauli-group elements under conjugation by the stabilizer gates [28].

For the CNOT case, subscript 1 indicates the control and 2 the target.

GATE	INPUT	OUTPUT	GATE	INPUT	OUTPUT
$H$	$X$	$Z$	$CNOT$	$I_1 X_2$	$I_1 X_2$
	$Y$	$-Y$		$X_1 I_2$	$X_1 X_2$
	$Z$	$X$		$I_1 Y_2$	$Z_1 Y_2$
$P$	$X$	$Y$		$Y_1 I_2$	$Y_1 X_2$
	$Y$	$-X$		$I_1 Z_2$	$Z_1 Z_2$
	$Z$	$Z$		$Z_1 I_2$	$Z_1 I_2$

$\mathcal{M}'$  is well-formed. It turns out that the Hadamard, Phase and CNOT gates (Figure 2a) as well as the Controlled-Z and Controlled-Y gates (Figure 4) have such mappings, i.e., these gates conjugate the Pauli group onto itself [17, 28]. Since these gates are directly simulated using stabilizers, they are commonly called *stabilizer gates*. Table 3 lists the transformation properties of Pauli literals under conjugation by the Hadamard, Phase and CNOT gates. Figure 4 shows that the Controlled-Z and Controlled-Y operations can be decomposed into Pauli, Hadamard and CNOT gates and thus are also stabilizer gates.

**Example 6.** Suppose we simulate a CNOT operation on  $|\psi\rangle = (|00\rangle + |11\rangle)/\sqrt{2}$  using  $\mathcal{M}$ ,

$$\mathcal{M} = \begin{array}{c|c} XX & \\ ZZ & \end{array} \xrightarrow{CNOT} \mathcal{M}' = \begin{array}{c|c} XI & \\ IZ & \end{array}$$

One can verify that the rows of  $\mathcal{M}'$  stabilize  $|\psi\rangle \xrightarrow{CNOT} (|00\rangle + |10\rangle)/\sqrt{2}$  as required.

The Hadamard, Phase and CNOT gates are also called *Clifford gates* because they generate the Clifford group of unitary operators. We use these names interchangeably. Any circuit composed exclusively of stabilizer gates is called a *unitary stabilizer circuit*. Table 3 shows that at most two columns of  $\mathcal{M}$  are updated when one simulates a stabilizer gate. Thus, such gates are simulated in  $\Theta(n)$  time.

**Theorem 7.** An  $n$ -qubit stabilizer state  $|\psi\rangle$  can be obtained by applying a stabilizer circuit to the  $|0\rangle^{\otimes n}$  computational-basis state.

**Proof.** The work in [2] represents the generators using a tableau, and then shows how to construct a unitary stabilizer circuit from the tableau. We refer the reader to [2, Theorem 8] for details of the proof.  $\square$

**Corollary 1.** An  $n$ -qubit stabilizer state  $|\psi\rangle$  can be transformed by stabilizer gates into the  $|00\dots 0\rangle$  computational-basis state.

**Proof.** Since every stabilizer state can be produced by applying some unitary stabilizer circuit  $\mathcal{C}$  to the  $|0\rangle^{\otimes n}$  state, it suffices to reverse  $\mathcal{C}$  to perform the inverse transformation. To reverse a stabilizer circuit, reverse the order of gates and replace every  $P$  gate with  $PPP$ .  $\square$

**Definition 3.** A pure state  $|\psi\rangle$  with computational-basis decomposition  $\sum_{k=0}^n \lambda_k |k\rangle$  is said to be *unbiased* if for all  $\lambda_i \neq 0$  and  $\lambda_j \neq 0$ ,  $|\lambda_i|^2 = |\lambda_j|^2$ . Otherwise, the state is *biased*.

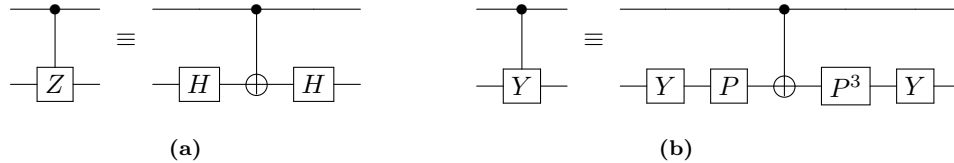


Fig. 4. Implementation of the (a) Controlled-Z and (b) Controlled-Y operations using Pauli and Clifford gates. These gates can be simulated directly on the stabilizer or using the equivalence shown here.

The stabilizer formalism also admits one-qubit measurements in the computational basis. However, the updates to  $\mathcal{M}$  for such gates are not as efficient as for stabilizer gates. Note that any qubit  $j$  in a stabilizer state is either in a  $|0\rangle$  ( $|1\rangle$ ) state or in an unbiased (Definition 3) superposition of both [17, 28, 32]. The former case is called a *deterministic outcome* and the latter a *random outcome*. We can tell these cases apart in  $\Theta(n)$  time by searching for  $X$  or  $Y$  literals in the  $j^{\text{th}}$  column of  $\mathcal{M}$ . If such literals are found, the qubit must be in a superposition and the outcome is random with equal probability ( $p(0) = p(1) = .5$ ); otherwise the outcome is deterministic ( $p(0) = 1$  or  $p(1) = 1$ ).

*Random case:* one flips an unbiased coin to decide the outcome and then updates  $\mathcal{M}$  to make it consistent with the outcome obtained. This requires at most  $n$  row multiplications leading to  $O(n^2)$  runtime [2, 28].

*Deterministic case:* no updates to  $\mathcal{M}$  are necessary but we need to figure out whether the state of the qubit is  $|0\rangle$  or  $|1\rangle$ , i.e., whether the qubit is stabilized by  $Z$  or  $-Z$ , respectively. One approach is to transform  $\mathcal{M}$  into row-echelon form using Algorithm 2.1. This removes redundant literals from  $\mathcal{M}$  in order to identify the row containing a  $Z$  in its  $j^{\text{th}}$  position and  $I$  everywhere else. The  $\pm$  phase of this row decides the outcome of the measurement. Since this approach is a form of Gaussian elimination, it takes  $O(n^3)$  time in practice (and can be completed asymptotically faster in theory).

Aaronson and Gottesman [2] improved the runtime of deterministic measurements by doubling the size of  $\mathcal{M}$  to include  $n$  *destabilizer generators* in addition to the  $n$  stabilizer generators. Such destabilizer generators help identify exactly which row multiplications to compute in order to decide the measurement outcome. This approach avoids Gaussian elimination, and thus deterministic measurements are computed in  $O(n^2)$  time.

When dealing with single-qubit  $Z$  measurements of the form  $P = Z \otimes I^{\otimes(n-1)}$ , we call the post-measurement states *cofactors*. Such states are separable stabilizer states of the form  $|0\rangle|\alpha_0\rangle$  and  $|1\rangle|\alpha_1\rangle$ . We denote the  $|0\rangle$ - and  $|1\rangle$ -cofactor by  $|\psi_{j=0}\rangle$  and  $|\psi_{j=1}\rangle$ , respectively, where  $j$  is the index of the measured qubit. The states  $|\alpha_0\rangle$  and  $|\alpha_1\rangle$  are called *reduced cofactors*, and are also stabilizer states. The generators of the reduced cofactors are obtained from the generators of the respective cofactors by dropping the generator added during measurement and removing from each remaining generator the  $Z$  literal at the  $j^{\text{th}}$  position.

**Definition 4.** Let  $|\psi\rangle = \sum_{k=0}^{2^n-1} \alpha_k |k\rangle$  and  $a \in \{0, 1\}$ . Furthermore, let  $C_{j=a}$  be the set of computational-basis states in  $|\psi\rangle$  with the  $j^{\text{th}}$  qubit set to  $a$  and  $\alpha_k \neq 0$ . The *support* of  $|\psi_{j=a}\rangle$ , denoted by  $|\psi_{j=a}|$ , is  $|C_{j=a}|$ .

**Observation 8.** The  $|0\rangle$ -cofactor of  $|\psi\rangle$ , with respect to qubit  $j$ , is  $|\psi_{j=0}\rangle = \sum_{|k\rangle \in C_{j=0}} \alpha_k |k\rangle$ . Similarly, the  $|1\rangle$ -cofactor of  $|\psi\rangle$ , with respect to  $j$ , is  $|\psi_{j=1}\rangle = \sum_{|k\rangle \in C_{j=1}} \alpha_k |k\rangle$ .

One can also consider *iterated cofactors*, such as *double cofactors*  $|\psi_{qr=00}\rangle \dots |\psi_{qr=11}\rangle$ . Cofactoring with respect to all qubits produces the individual amplitudes of the computational-basis states. The work in [32] establishes an alternative representation for stabilizer states that tracks the non-zero amplitudes of a stabilizer state using linear transformations and bilinear forms over the two-element field.

**Theorem 9.** [32, Appendix A] For an  $n$ -qubit stabilizer state  $|\psi\rangle$ ,  $\exists \mathbf{c}, \mathbf{t} \in \mathbb{Z}_2^n$ ,  $\mathbf{R}$  an  $n \times k$  binary matrix with column rank  $k \leq n$ , and  $n \times n$  symmetric binary matrix  $\mathbf{Q}$ , such that

$$|\psi\rangle = \frac{1}{2^{k/2}} \sum_{\mathbf{x} \in \mathbb{Z}_2^k} i^{2\mathbf{c}^\top \mathbf{y} + \mathbf{y}^\top \mathbf{Q} \mathbf{y}} |\mathbf{y} = \mathbf{R}\mathbf{x} + \mathbf{t}\rangle \quad (2)$$

**Corollary 2.** The basis amplitudes of a stabilizer state  $|s\rangle$  have the following properties:

- (i) The number of non-zero amplitudes (support) in  $|s\rangle$  is a power of two.
- (ii) State  $|s\rangle$  is unbiased, and every non-zero amplitude is  $\frac{\pm 1}{\sqrt{|s|}}$  or  $\frac{\pm i}{\sqrt{|s|}}$ , where  $|s|$  is the support of  $|s\rangle$ .
- (iii) The number of imaginary amplitudes in  $|s\rangle$  is either zero or half the number of non-zero amplitudes.<sup>g</sup>
- (iv) The number of negative amplitudes in  $|s\rangle$  is either zero or a power of two.<sup>h</sup>
- (v) For each qubit  $q$  of  $|s\rangle$ , the number of basis states with  $q = 0$  in the  $|0\rangle$ - and  $|1\rangle$ -cofactors is either zero or a power of two. Furthermore, if both  $|0\rangle$ - and  $|1\rangle$ -cofactors with respect to a given qubit are nontrivial, the supports of the cofactors must be equal and the norms of the cofactors must be equal.

Corollary 2 is illustrated in Table 2 and Appendix A. Its further implications are discussed in Section 3. Corollary 2-v is restated as Lemma 4 and proven in Section 4.2.

### 3 Geometric Properties of Stabilizer States

Given  $\langle\psi|\varphi\rangle = re^{i\alpha}$ , we normalize the global phase of  $|\psi\rangle$  to ensure, without loss of generality, that  $\langle\psi|\varphi\rangle \in \mathbb{R}_+$ .

**Theorem 10.** Let  $S(|\psi\rangle)$  and  $S(|\varphi\rangle)$  be the stabilizer groups for  $|\psi\rangle$  and  $|\varphi\rangle$ , respectively. If there exist  $P \in S(|\psi\rangle)$  and  $Q \in S(|\varphi\rangle)$  such that  $P = -Q$ , then  $|\psi\rangle \perp |\varphi\rangle$ .

**Proof.** Since  $|\psi\rangle$  is a 1-eigenvector of  $P$  and  $|\varphi\rangle$  is a  $(-1)$ -eigenvector of  $P$ , they must be orthogonal.  $\square$

**Theorem 11.** [2] Let  $|\psi\rangle, |\varphi\rangle$  be oblique stabilizer states. Let  $s$  be the minimum, over all sets of generators  $\{P_1, \dots, P_n\}$  for  $S(|\psi\rangle)$  and  $\{Q_1, \dots, Q_n\}$  for  $S(|\varphi\rangle)$ , of the number of different  $i$  values for which  $P_i \neq Q_i$ . Then,  $|\langle\psi|\varphi\rangle| = 2^{-s/2}$ .

**Proof.** Since  $\langle\psi|\varphi\rangle$  is not affected by unitary transformations  $U$ , we choose a stabilizer circuit such that  $U|\psi\rangle = |b\rangle$ , where  $|b\rangle$  is a basis state. For this state, select the stabilizer generators  $\mathcal{M}$  of the form  $I \dots IZI \dots I$ . Perform Gaussian elimination on  $\mathcal{M}$  to minimize the incidence of  $P_i \neq Q_i$ . Consider two cases. If  $U|\varphi\rangle \neq |b\rangle$  and its generators contain only  $I/Z$  literals, then  $U|\varphi\rangle \perp U|\psi\rangle$ , which contradicts the assumption that  $|\psi\rangle$  and  $|\varphi\rangle$  are oblique. Otherwise, each generator of  $U|\varphi\rangle$  containing  $X/Y$  literals contributes a factor of  $1/\sqrt{2}$  to the inner product.  $\square$

**Corollary 3.** Let  $|\psi\rangle$  and  $|\phi\rangle$  be oblique  $n$ -qubit stabilizer states such that  $|\psi\rangle \neq e^{i\alpha}|\phi\rangle$ . Then,  $2^{-n/2} \leq |\langle\psi|\phi\rangle| \leq 2^{-1/2}$ .

<sup>g</sup> Assuming the amplitudes are normalized such that the first non-zero basis amplitude is 1.0.

<sup>h</sup> For normalized amplitudes, this might require multiplying by a  $-1$  global phase.

### 3.1 Inner products and $k$ -neighbor stabilizer states

**Definition 5.** Given an arbitrary state  $|\psi\rangle$  with  $\|\psi\| = 1$ , a stabilizer state  $|\varphi\rangle$  is a  $k$ -neighbor stabilizer state of  $|\psi\rangle$  if  $|\langle\psi|\varphi\rangle| = 2^{-k/2}$ .

When two stabilizer states are 1-neighbors we will also refer to them as *nearest neighbors* since, by Corollary 3, this is the maximal inner-product value  $\neq 1$ . Furthermore, the distance between a stabilizer state and any of its  $k$ -neighbors is  $\sqrt{2 - 2^{1-k/2}}$ . Therefore, the distance between closest stabilizer states (nearest neighbors) is  $\sqrt{2 - \sqrt{2}} \approx 0.765$ .

**Proposition 12.** Consider two orthogonal stabilizer states  $|\alpha\rangle$  and  $|\beta\rangle$  whose unbiased superposition  $|\psi\rangle$  is also a stabilizer state. Then  $|\psi\rangle$  is a nearest neighbor of  $|\alpha\rangle$  and  $|\beta\rangle$ .

**Proof.** Since stabilizer states are unbiased,  $|\langle\psi|\alpha\rangle| = |\langle\psi|\beta\rangle| = \frac{1}{\sqrt{2}}$ . Thus,  $|\psi\rangle$  is a 1-neighbor or nearest-neighbor stabilizer state to  $|\alpha\rangle$  and  $|\beta\rangle$ . Figure 1 illustrates this case.  $\square$

**Lemma 1.** Any two stabilizer states have equal numbers of  $k$ -neighbor stabilizer states.

**Proof.** Any stabilizer state can be mapped to another stabilizer state by a stabilizer circuit (Corollary 1). Since such circuits effect unitary operators, inner products are preserved.  $\square$

**Lemma 2.** Let  $|\psi\rangle$  and  $|\varphi\rangle$  be  $n$ -qubit stabilizer states such that  $\langle\psi|\varphi\rangle \neq 1$ . Then  $\frac{|\psi\rangle + i^l |\varphi\rangle}{\sqrt{2}}$ ,  $l \in \{0, 1, 2, 3\}$ , is a stabilizer state iff  $\langle\psi|\varphi\rangle = 0$  and  $|\varphi\rangle = P|\psi\rangle$ , where  $P \in \mathcal{G}_n$ .

**Proof.** We first prove that, if  $\langle\psi|\varphi\rangle = 0$  and  $|\varphi\rangle = P|\psi\rangle$ , an unbiased sum of such states is also a stabilizer state. Suppose  $S(|\psi\rangle) = \langle g_k \rangle_{k=1,2,\dots,n}$  is generated by elements  $g_k$  of the  $n$ -qubit Pauli group. Let

$$f(k) = \begin{cases} 0 & \text{if } [P, g_k] = 0 \\ 1 & \text{otherwise} \end{cases}$$

and write  $S(|\varphi\rangle) = \langle (-1)^{f(k)} g_k \rangle$ . Conjugating each generator  $g_k$  by  $P$  we see that  $|\varphi\rangle$  is stabilized by  $\langle (-1)^{f(k)} g_k \rangle$ . Let  $Z_k$  (respectively  $X_k$ ) denote the Pauli operator  $Z$  ( $X$ ) acting on the  $k^{\text{th}}$  qubit. By Corollary 1, there exists an element  $\mathcal{C}$  of the  $n$ -qubit Clifford group which maps  $S(|\psi\rangle)$  to basis form (Definition 2) such that  $\mathcal{C}|\psi\rangle = |0\rangle^{\otimes n}$  and  $\mathcal{C}|\varphi\rangle = (\mathcal{C}P\mathcal{C}^\dagger)\mathcal{C}|\psi\rangle = i^m |f(1)f(2)\dots f(n)\rangle$ . The second equality follows from the fact that  $\mathcal{C}P\mathcal{C}^\dagger$  is an element of the Pauli group and can therefore be written as  $i^m X(v)Z(u)$  for some  $m \in \{0, 1, 2, 3\}$  and  $u, v \in \mathbb{Z}_2^k$ . Therefore,

$$\frac{|\psi\rangle + i^l |\varphi\rangle}{\sqrt{2}} = \frac{\mathcal{C}^\dagger(|0\rangle^{\otimes n} + i^{t=(l+m) \bmod 4} |f(1)f(2)\dots f(n)\rangle)}{\sqrt{2}} \quad (3)$$

The state in parentheses on the right-hand side is the product of an all-zeros state and a GHZ state. Therefore, the sum is stabilized by  $S' = \mathcal{C}^\dagger \langle S_{\text{zero}}, S_{\text{ghz}} \rangle \mathcal{C}$  where  $S_{\text{zero}} = \langle Z_i, i \in \{k | f(k) = 0\} \rangle$  and  $S_{\text{ghz}}$  is supported on  $\{k | f(k) = 1\}$  and equals  $\langle (-1)^{t/2} X X \dots X, \forall i Z_i Z_{i+1} \rangle$  if  $t = 0 \bmod 2$  or  $\langle (-1)^{(t-1)/2} Y Y \dots Y, \forall i Z_i Z_{i+1} \rangle$  if  $t = 1 \bmod 2$ .

We now prove the opposite implication. Let  $|u\rangle = \frac{|\psi\rangle + i^l |\varphi\rangle}{\sqrt{2}}$ , where  $|\psi\rangle$  and  $|\varphi\rangle$  are  $n$ -qubit stabilizer states and  $\langle\psi|\varphi\rangle \neq 1$ . Let  $\mathcal{C}_1$  and  $\mathcal{C}_2$  be Clifford circuits such that  $|\psi\rangle = \mathcal{C}_1 |\mathbf{0}\rangle$  and  $|\varphi\rangle = \mathcal{C}_2 |\mathbf{0}\rangle$ , where  $|\mathbf{0}\rangle = |0\rangle^{\otimes n}$ . Observe that  $\mathcal{C}_1 \neq \mathcal{C}_2$  by our assumption that  $\langle\psi|\varphi\rangle \neq 1$ . Therefore,  $|u\rangle = (\mathcal{C}_1 |\mathbf{0}\rangle + i^l \mathcal{C}_2 |\mathbf{0}\rangle) / \sqrt{2} = \mathcal{C}_1 (|\mathbf{0}\rangle + i^l \mathcal{C}_1^\dagger \mathcal{C}_2 |\mathbf{0}\rangle) / \sqrt{2}$ , and

$$\mathcal{C}_1^\dagger |u\rangle = \frac{|\mathbf{0}\rangle + i^l \mathcal{C}_1^\dagger \mathcal{C}_2 |\mathbf{0}\rangle}{\sqrt{2}}$$

Since  $\mathcal{C}_1^\dagger \mathcal{C}_2 \neq I^{\otimes n}$  and  $\mathcal{C}_1^\dagger |u\rangle$  is a stabilizer state,  $\mathcal{C}_1^\dagger \mathcal{C}_2 |\mathbf{0}\rangle$  must simplify to a basis state  $|b\rangle \neq |\mathbf{0}\rangle$  (otherwise,  $\mathcal{C}_1^\dagger |u\rangle$  is either biased or has  $2^n - 1$  basis states). It follows that,

$\langle \psi | \varphi \rangle = \langle \mathbf{0} | \mathcal{C}_1^\dagger \mathcal{C}_2 | \mathbf{0} \rangle = \langle \mathbf{0} | b \rangle = 0$ . Let  $i^l |b\rangle = P | \mathbf{0} \rangle$ , where  $P$  is an element of the Pauli group,

$$\begin{aligned} \mathcal{C}_1^\dagger |u\rangle &= | \mathbf{0} \rangle + P | \mathbf{0} \rangle \\ |u\rangle &= \mathcal{C}_1 | \mathbf{0} \rangle + \mathcal{C}_1 P | \mathbf{0} \rangle = \mathcal{C}_1 | \mathbf{0} \rangle + (\mathcal{C}_1 P \mathcal{C}_1^\dagger) \mathcal{C}_1 | \mathbf{0} \rangle \\ &= \mathcal{C}_1 | \mathbf{0} \rangle + P' \mathcal{C}_1 | \mathbf{0} \rangle = | \psi \rangle + P' | \psi \rangle \quad \square \end{aligned}$$

**Corollary 4.** *Let  $\frac{|\psi\rangle + i^l |\varphi\rangle}{\sqrt{2}}$  be a stabilizer state. Then the canonical stabilizer matrices for  $|\psi\rangle$  and  $|\varphi\rangle$  are similar.*

**Proof.** Let  $\mathcal{M}^\psi = \{R_1, R_2, \dots, R_n\}$  be the canonical stabilizer matrix for  $|\psi\rangle$ . Since  $|\varphi\rangle = P |\psi\rangle$  by Lemma 2,  $\mathcal{M}^\varphi = \{(-1)^c R_1, (-1)^c R_2, \dots, (-1)^c R_n\}$ , where  $c = 0$  if  $P$  and  $R_i$  commute, and  $c = 1$  otherwise.  $\square$

**Theorem 13.** *For any  $n$ -qubit stabilizer state  $|\psi\rangle$ , there are  $4(2^n - 1)$  nearest-neighbor stabilizer states, and these states can be produced as described in Lemma 2.*

**Proof.** The all-zeros basis amplitude of any stabilizer state  $|\psi\rangle$  that is a nearest neighbor to  $|0\rangle^{\otimes n}$  must be  $\propto 1/\sqrt{2}$ . Therefore,  $|\psi\rangle$  is an unbiased superposition of  $|0\rangle^{\otimes n}$  and one of the other  $2^n - 1$  basis states, i.e.,  $|\psi\rangle = \frac{|0\rangle^{\otimes n} + P|0\rangle^{\otimes n}}{\sqrt{2}}$ , where  $P \in \mathcal{G}_n$  such that  $P|0\rangle^{\otimes n} \neq \alpha|0\rangle^{\otimes n}$ .

As in the proof of Lemma 2, we have  $|\psi\rangle = \frac{|0\rangle^{\otimes n} + i^l |\varphi\rangle}{\sqrt{2}}$ , where  $|\varphi\rangle$  is a basis state and  $l \in \{0, 1, 2, 3\}$ . Thus, there are 4 possible unbiased superpositions, and a total of  $4(2^n - 1)$  nearest-neighbor stabilizer states. Since  $|0\rangle^{\otimes n}$  is a stabilizer state, all stabilizer states have the same number of nearest neighbors by Lemma 1.  $\square$

**Corollary 5.** *For any  $n$ -qubit stabilizer state  $|\psi\rangle$ , there exists a set of states  $V_\psi = \{|s_i\rangle\}_{i=1}^{2^n-1}$  such that each  $|s_i\rangle$  is a nearest-neighbor to  $|\psi\rangle$  and  $\langle s_i | s_j \rangle = 1/2$  for  $i \neq j$ . This set  $V_\psi$  together with  $|\psi\rangle$  form a basis in  $\mathcal{H}^{\otimes n}$ .*

**Proof.** Without loss of generality, assume that  $|\psi\rangle = |0\rangle^{\otimes n}$ . Theorem 13 shows that, for any given stabilizer states, its nearest neighbors come in groups of four. Taking any one representative from each group of four, we get a set of states  $V_\psi = \left\{ |s_i\rangle = \frac{|0\rangle^{\otimes n} + i^l |b_i\rangle}{\sqrt{2}} \right\}_{i=1}^{2^n-1}$ , where  $l \in \{0, 1, 2, 3\}$  and  $|b_i\rangle$  are computational-basis states other than  $|\psi\rangle$ . Thus, for all  $|s_i\rangle$  and  $|s_j\rangle$  such that  $i \neq j$ ,

$$\langle s_i | s_j \rangle = \left( \frac{\langle 0^{\otimes n} | + \langle b_i |}{\sqrt{2}} \right) \left( \frac{|0^{\otimes n}\rangle + |b_j\rangle}{\sqrt{2}} \right) = \frac{1}{2} \quad (4)$$

$V_\psi$  together with  $|\psi\rangle$  form a linearly independent set (one can subtract  $|\psi\rangle$  from each  $|s_i\rangle$  to get an orthogonal set) and thus a basis. Figure 1 illustrates this nearest-neighbor structure for a small set of states.  $\square$

In Table 2, one can find the twelve nearest-neighbor states of  $|00\rangle$ . We computed the angles between all-pairs of 3-qubit stabilizer states and confirmed that each was surrounded by exactly 28 nearest neighbors. The same procedure confirmed that the number of nearest neighbors for any 4-qubit stabilizer state is 60. In Section 5.3, we describe an orthogonalization procedure for linear combinations of stabilizer states that takes advantage of the nearest-neighbor structure described in Theorem 13.

Alternatively, Theorem 13 can also be proven using a counting argument. By Theorem 11, we know that any nearest-neighbor stabilizer state to  $|0^{\otimes n}\rangle$  can be represented by a stabilizer matrix that has exactly one generator (row) with at least one  $X/Y$  literal. Therefore, there

are  $2(4^n - 2^n)$  choices for the first generator  $P_1$ . The factor of 2 accounts for the possible signs of  $P_1$ . The remaining (independent) generators,  $P_2, \dots, P_n$ , are then selected such that they commute with  $P_1$  and consist of  $Z/I$  literals only. Observe that such generators can be selected arbitrarily since they generate the same  $(Z/I)$ -element subgroup.

**Example 14.** Suppose  $P_1 = XII$ , then  $P_2$  and  $P_3$  can be selected arbitrarily from the set  $\{IZI, IZZ, IIZ\}$ . To account for stabilizer matrices that describe the same state, consider that  $P_1$  can be replaced by  $P_1Q$ , where  $Q$  is an arbitrary product of the  $Z/I$  generators.

Therefore, the number of nearest-neighbor stabilizer states  $\mathcal{L}_n(1)$  is given by,

$$\mathcal{L}_n(1) = \frac{2(4^n - 2^n)}{2^{n-1}} = 4(2^n - 1) \quad (5)$$

The following theorem generalizes Equation 5 to the case of  $k$ -neighbor stabilizer states.

**Theorem 15.** *For any  $n$ -qubit stabilizer state, the number of  $k$ -neighbor stabilizer states is,*

$$\mathcal{L}_n(k) = 2^{k(k+1-n)} \prod_{j=0}^{k-1} \frac{4^n/2^j - 2^n}{2^k - 2^j} \quad (6)$$

**Proof.** Without loss of generality, we count the  $k$ -neighbors of  $|0^{\otimes n}\rangle$  (Lemma 1). By Theorem 11, we know that such states are represented by an  $n$ -qubit stabilizer matrix with  $k$  independent  $X/Y$  generators and  $n - k$  independent  $Z/I$  generators. Assume, for  $j \leq k$ , that the  $X/Y$  generators  $P_1, \dots, P_{j-1}$  have been chosen, and let  $Q_j, \dots, Q_n$  be  $Z/I$  generators that commute with them. Given this generating set, we count the possible choices for  $P_j$  to replace any one of the  $Z/I$  generators. Observe that,  $P_j$  must commute with  $P_1, \dots, P_{j-1}$  and cannot be an element of the subgroup generated by  $P_1, \dots, P_{j-1}, Q_j, \dots, Q_n$ . Thus, there are  $2(4^n/2^{j-1} - 2^n)$  choices for  $P_j$ . The factor of 2 accounts for the choice of sign. We need to account for choices of  $X/Y$  generators that describe the same state. Consider the subgroup generated by  $P_{i \in \{1, \dots, k\}}$ . There are  $2^k - 1$  choices for  $P_1$ ,  $2^k - 2$  for  $P_2$ ,  $2^k - 4$  for  $P_3$ , and so on. This gives a factor of  $\prod_{j=1}^k (2^k - 2^{j-1})$ . Furthermore, we can replace  $P_i$  by  $P_iQ$ , where  $Q$  is an arbitrary product of the  $Z/I$  generators. This gives  $k$  factors of  $2^{n-k}$ .

$$\mathcal{L}_n(k) = \prod_{j=1}^k \frac{2}{2^{n-k}} \frac{4^n/2^{j-1} - 2^n}{2^k - 2^{j-1}} \quad \square$$

**Corollary 6.** *For an arbitrary  $n$ -qubit stabilizer state  $|\psi\rangle$ , the number of stabilizer states orthogonal to  $|\psi\rangle$  is,*

$$\mathcal{L}_n(\perp) = \mathcal{N}(n) - \sum_{k=1}^n \mathcal{L}_n(k) - 1 = \frac{\mathcal{N}(n)(2^n - 1)}{3 \cdot 2^n} \quad (7)$$

where  $\mathcal{N}(n)$  is the number of  $n$ -qubit stabilizer states (Proposition 2). In other words, for any  $n$ -qubit stabilizer state  $|\psi\rangle$  with a sufficiently large  $n$ , almost  $1/3$  of remaining stabilizer states are orthogonal to  $|\psi\rangle$ .

As an illustration of Theorem 15 and Corollary 6, Table 4 numerically describes the distribution of inner products between any one  $n$ -qubit stabilizer state and all other stabilizer states for  $n \in \{1, \dots, 7\}$ . This table shows that the number of nearest-neighbor stabilizer

states as a fraction of all  $n$ -qubit stabilizer states approaches zero as  $n$  increases. We now formalize other trends gleaned from Table 4.

**Lemma 3.** *For an arbitrary  $n$ -qubit stabilizer state, consider the quantity  $a_{n,k} = \frac{\mathcal{L}_n(k)}{\mathcal{N}(n)}$ , where  $0 < k \leq n$ . Then, for fixed  $m$ , the sequence  $\{a_{n,n-m}\}^{n \rightarrow \infty}$  is monotonically convergent.*

**Proof.** Using Theorem 15 and the recurrence relation of Equation 1 we obtain,

$$\frac{a_{n,k}}{a_{n+1,k+1}} = \frac{\mathcal{L}_n(k)}{\mathcal{N}(n)} \cdot \frac{2(2^{n+1} + 1)\mathcal{N}(n)}{\mathcal{L}_{n+1}(k+1)} = 2(2^{n+1} + 1) \frac{\mathcal{L}_n(k)}{\mathcal{L}_{n+1}(k+1)} \quad (8)$$

where

$$\begin{aligned} \frac{\mathcal{L}_n(k)}{\mathcal{L}_{n+1}(k+1)} &= 2^{n-k-1} \prod_{j=0}^{k-1} \left( \frac{4^n/2^j - 2^n}{2^k - 2^j} \right) \prod_{j=0}^k \left( 2 \frac{2^k - 2^{j-1}}{4^{n+1}/2^j - 2^{n+1}} \right) \\ &= 2^n \prod_{j=1}^k \left( \frac{4^n/2^{j-1} - 2^n}{2^k - 2^{j-1}} \right) \prod_{j=0}^k \left( \frac{2^k - 2^{j-1}}{4^{n+1}/2^j - 2^{n+1}} \right) \\ &= 2^n \left( \frac{2^k - 1/2}{4^{n+1} - 2^{n+1}} \right) \prod_{j=1}^k \left( \frac{1}{2} \frac{4^n/2^{j-1} - 2^n}{2(4^n/2^j - 2^n)} \right) = \frac{2^{k+1} - 1}{2^k(2^{n+3} - 4)} \end{aligned}$$

Inserting the above result in Equation 8 gives,

$$\frac{a_{n,k}}{a_{n+1,k+1}} = 2(2^{n+1} + 1) \frac{2^{k+1} - 1}{2^k(2^{n+3} - 4)} = \frac{2^{n+k+3} + 2^{k+2} - 2^{n+2} - 2}{2^{n+k+3} - 2^{k+2}} \quad (9)$$

Consider the case  $0 < k < n$ ,

$$\frac{2^{n+k+3} + 2^{k+2} - 2^{n+2} - 2}{2^{n+k+3} - 2^{k+2}} < 1 \quad \text{and thus} \quad \frac{2^{k+2}}{2^{n+1} + 1} < 1$$

Therefore, for fixed  $0 < m < n$ ,  $\{a_{n,n-m}\}^{n \rightarrow \infty}$  is monotonically increasing. It converges because  $0 < a_{n,k} < 1$ . For the case  $k = n$ ,

$$\frac{a_{n,n}}{a_{n+1,n+1}} = \frac{2^{2n+3} - 2}{2^{2n+3} - 2^{n+2}} = \frac{2^{n+1} - 2^{-n-1}}{2^{n+1} - 1} = 1 + \frac{1}{2^{n+1}} > 1 \quad (10)$$

Therefore, the sequence  $\{a_{n,n}\}^{n \rightarrow \infty}$  is monotonically decreasing and convergent.  $\square$

Table 4. Distribution of inner products (angles) between any one  $n$ -qubit stabilizer state and all other stabilizer states for  $n \in \{1, \dots, 7\}$ . The last column indicates the ratio of orthogonal ( $\perp$ ) states.

$n$	$\mathcal{N}(n)$	$\mathcal{L}_n(k)/(\mathcal{N}(n) - 1)$							
		$k = 1$ (45.00°)	$k = 2$ (60.00°)	$k = 3$ (69.30°)	$k = 4$ (75.52°)	$k = 5$ (79.82°)	$k = 6$ (82.82°)	$k = 7$ (84.93°)	$\perp$ (90.00°)
1	6	80%							20%
2	60	20.34%	54.24%						25.42%
3	1080	2.59%	20.76%	47.45%					29.19%
4	36720	0.16%	3.05%	20.92%	44.62%				31.25%
5	2423520	0.01%	0.20%	3.27%	20.96%	43.27%			32.29%
6	315057600	$\approx 0\%$	0.01%	0.23%	3.39%	20.97%	42.60%		32.81%
7	81284860800	$\approx 0\%$	$\approx 0\%$	0.01%	0.24%	3.44%	20.97%	42.27%	33.07%



**Theorem 16.** For an arbitrary  $n$ -qubit stabilizer state, the limit of the sequence  $\{a_{n,n-k}\}^{n \rightarrow \infty}$ ,  $0 \leq k < n$ , lies in the interval  $[l(k), u(k)]$ , where

$$l(k) = \frac{M_5}{2^{k(k+5)/2}} \cdot \exp\left(\frac{1}{32} - \frac{2}{2^{k+5} - 1}\right) \quad u(k) = \frac{M_5}{2^{k(k+3)/2}} \cdot \exp\left(\frac{1}{15} - \frac{2}{2^{k+5} + 1}\right)$$

and

$$M_5 = \prod_{j=1}^5 \left(\frac{1}{1 - 2^{-j}}\right) \prod_{j=1}^5 \left(1 - \frac{2}{2^{j+k} + 1}\right)$$

**Proof.** From the proof of Lemma 3 we know  $0 < l(k) < u(k) < 1$ . We now derive the sharper bounds,  $l(k)$  and  $u(k)$ , for  $\{a_{n,n-k}\}^{n \rightarrow \infty}$ . Using Theorem 15 and Proposition 2 we obtain,

$$a_{n,n-k} = 2^{-k} \underbrace{\prod_{j=1}^{n-k} \left(\frac{1}{1 - 2^{-j}}\right)}_{A_{n-k}} \underbrace{\prod_{j=1}^{n-k} \left(1 - \frac{2}{2^{j+k} + 1}\right)}_{B_{n-k}} \underbrace{\prod_{j=1}^k \left(\frac{1}{1 + 2^j}\right)}_{C_k} \quad (11)$$

We now derive upper and lower bounds for the products  $A_{n-k}$ ,  $B_{n-k}$  and  $C_k$ .

$$\begin{aligned} \prod_{j=1}^{n-k} \exp\left(\frac{1}{2^j}\right) &< A_{n-k} < \prod_{j=1}^{n-k} \exp\left(\frac{1}{2^j - 1}\right) \\ \prod_{j=1}^{n-k} \exp\left(\frac{-2}{2^{j+k} - 1}\right) &< B_{n-k} < \prod_{j=1}^{n-k} \exp\left(\frac{-2}{2^{j+k} + 1}\right) \\ \frac{1}{2^{k(k+5)/2}} &= \prod_{j=1}^k \frac{1}{2^{j+1}} < C_k < \prod_{j=1}^k \frac{1}{2^j} = \frac{1}{2^{k(k+1)/2}} \end{aligned}$$

Therefore, as  $n \rightarrow \infty$ ,

$$\begin{aligned} A_5 \cdot \exp\left(\frac{1}{32}\right) &< A_\infty < A_5 \cdot \exp\left(\frac{1}{15}\right) \\ B_5 \cdot \exp\left(\frac{-2}{2^{j+k} - 1}\right) &< B_\infty < B_5 \cdot \exp\left(\frac{-2}{2^{j+k} + 1}\right) \quad \square \end{aligned}$$

In particular, observe that  $u(k) \approx 0$  for  $k > 4$ . Thus, the fraction of all stabilizer states that are oblique to some  $n$ -qubit stabilizer state  $|\psi\rangle$  is dominated by its  $(n-k)$ -neighbors, where  $k \in \{0, 1, 2, 3, 4\}$ . Limit values for  $\mathcal{L}_n(n-k)/\mathcal{N}(n)$  are approximated in Figure 5-a.

**Theorem 17.** For two  $n$ -qubit stabilizer states  $|\psi\rangle$  and  $|\phi\rangle$  drawn independently from a uniform distribution, the expected value  $E[\langle\psi|\phi\rangle] \rightarrow 0$  as  $n \rightarrow \infty$ .

**Proof.** Let  $|\varphi_{n-k}\rangle$  be an  $(n-k)$ -neighbor of  $|\psi\rangle$ . By Theorems 11 and 16,

$$E[\langle\psi|\phi\rangle] = \sum_{k=0}^{n-1} a_{n,n-k} |\langle\psi|\varphi_{n-k}\rangle| < \sum_{k=0}^{n-1} u(k) |\langle\psi|\varphi_{n-k}\rangle| \approx \sum_{k=0}^4 u(k) 2^{(k-n)/2} \quad (12)$$

Therefore,  $E_\infty[\langle\psi|\phi\rangle] < \sum_{k=0}^4 u(k) 2^{(k-n)/2}$ , which approaches zero as  $n \rightarrow \infty$ .  $\square$

Theorem 17 suggests that stabilizer states are distributed in a way similar to random quantum states [11, 24, 26].

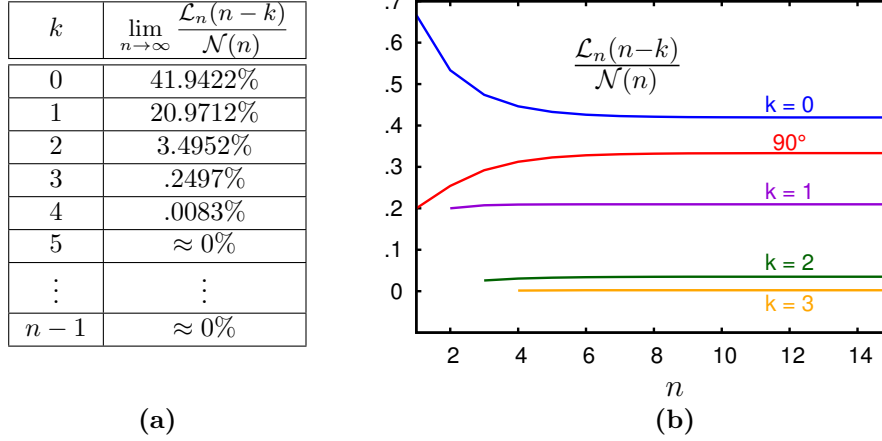


Fig. 5. **(a)** For an  $n$ -qubit stabilizer state  $|\psi\rangle$ , the fraction ( $\approx 2/3$ ) of all stabilizer states that are oblique to  $|\psi\rangle$  is dominated by its  $(n-k)$ -neighbors, where  $k \in \{0, 1, 2, 3, 4\}$ . **(b)** The stabilizer states orthogonal to  $|\psi\rangle$  together with its  $(n-k)$ -neighbors ( $k < 3$ ) account for  $\approx 99\%$  of all states.

### 3.2 Exterior products and stabilizer bivectors

In this section, we study pairs of stabilizer states and the parallelograms they form, which lie in a  $2n$ -qubit Hilbert space. Such pairs of states are called *bivectors* and are obtained by computing the wedge product  $|\psi \wedge \phi\rangle = |\psi\rangle \otimes |\phi\rangle - |\phi\rangle \otimes |\psi\rangle$  between stabilizer states. The wedge product is antisymmetric and yields zero for parallel vectors. The norm of a stabilizer bivector can be interpreted as the *signed area* of the parallelogram defined by non-parallel stabilizer states.

**Definition 6.** A *stabilizer bivector*  $|\varphi\rangle$  is a  $2n$ -qubit stabilizer state such that  $|\varphi\rangle \propto |\psi \wedge \phi\rangle$ , where  $|\psi\rangle$  and  $|\phi\rangle$  are  $n$ -qubit stabilizer states.

**Example 18.** The wedge product of the stabilizer states  $|\psi\rangle = |00\rangle + |11\rangle$  and  $|\phi\rangle = |00\rangle - |11\rangle$  produces the stabilizer bivector  $|\psi \wedge \phi\rangle = |1100\rangle + |0011\rangle$  (up to a phase). In contrast, given the states  $|\psi\rangle = |00\rangle + |11\rangle$  and  $|\phi\rangle = |10\rangle$ ,  $|\psi \wedge \phi\rangle = |0010\rangle + |1100\rangle + |1110\rangle - |0011\rangle - |1000\rangle - |1011\rangle$  is not a stabilizer bivector because the number of constituent basis states is not a power of two (Corollary 2-ii).

The work in [14, 22] derives measures of entanglement for general pure bipartite states based on the alternating tensor product space defined by the wedge product of two states. Furthermore, Hayashi et al. [20] conclude that the antisymmetric basis states (the wedge product of basis states) are more entangled than any symmetric basis states. Therefore, stabilizer bivectors are potential candidates for developing new entanglement monotones for quantifying quantum resources. In Section 5.4, we describe how to efficiently compute a generator set for stabilizer bivectors.

**Theorem 19.** For any  $n$ -qubit stabilizer state  $|\psi\rangle$ , there are at least  $5(2^n - 1)$  distinct stabilizer states  $|\phi\rangle$  such that the wedge product  $|\psi \wedge \phi\rangle$  is a stabilizer bivector.

**Proof.** By Proposition 3,  $|\psi\rangle|\phi\rangle$  and  $|\phi\rangle|\psi\rangle$  are both stabilizer states. Consider two cases.

*Case 1:*  $|\psi\rangle$  and  $|\phi\rangle$  are orthogonal. From Lemma 2 and Corollary 4 we know that, if  $|\psi\rangle|\phi\rangle - |\phi\rangle|\psi\rangle$  is a stabilizer state, the canonical matrices of  $|\psi\rangle$  and  $|\phi\rangle$  must be *similar* (Definition 1). Since each *dissimilar* matrix (Definition 1) can be used to represent  $2^n$  states

(the number of possible phase-vector permutations) and  $|\psi \wedge \psi\rangle = 0$ , there are  $2^n - 1$  such wedge products that produce stabilizer bivectors.

*Case 2:*  $|\psi\rangle$  and  $|\phi\rangle$  are 1-neighbors. By Theorem 13,  $|\psi\rangle = \frac{|\phi\rangle + P|\phi\rangle}{\sqrt{2}}$  and  $|\phi\rangle = \frac{|\psi\rangle + P'|\psi\rangle}{\sqrt{2}}$ , where  $P$  and  $P'$  are Pauli operators. Therefore,

$$|\psi \wedge \phi\rangle = \left( \frac{|\phi\rangle + P|\phi\rangle}{\sqrt{2}} \right) \wedge |\phi\rangle = \frac{(P|\phi\rangle) \wedge |\phi\rangle}{\sqrt{2}} \quad (13)$$

Since  $|\phi\rangle$  and  $P|\phi\rangle$  are orthogonal with similar stabilizer matrices (Case 1),  $|\psi \wedge \phi\rangle$  is a stabilizer bivector (up to a normalizing factor), and there are  $4(2^n - 1)$  such wedge products.

We now show that for  $k$ -neighbors  $|\psi\rangle$  and  $|\phi\rangle$ ,  $k > 1$ ,  $|\psi \wedge \phi\rangle$  is not a stabilizer bivector. Without loss of generality, let  $|\psi\rangle = |0\rangle$  and  $|\phi\rangle = \sum_{i=0}^{2^k-1} \alpha_i |b_i\rangle$ , where the  $|b_i\rangle$  are computational-basis states.

$$|\psi \wedge \phi\rangle = |0\rangle \wedge \left( \sum_{i=0}^{2^k-1} \alpha_i |b_i\rangle \right) = \sum_{i=1}^{2^k-1} |0 \wedge b_i\rangle \quad (14)$$

Therefore,  $|\psi \wedge \phi\rangle$  has  $2^{k+1} - 2$  computational-basis states, which is not a power of 2 for  $k > 1$ . By Corollary 2-i,  $|\psi \wedge \phi\rangle$  is not a stabilizer bivector for  $(k > 1)$ -neighbors.  $\square$

**Proposition 20.** *Given any two  $n$ -qubit stabilizer states  $|\psi\rangle$  and  $|\phi\rangle$ , the area of the parallelogram formed by these states is  $\|\psi \wedge \phi\| = \sqrt{1 - 2^{-k}}$ ,  $0 \leq k \leq n$ .*

**Proof.** Consider the determinant of the *Gramian matrix* of the states,

$$\det \begin{vmatrix} 1 & \langle \psi | \phi \rangle \\ \langle \phi | \psi \rangle & 1 \end{vmatrix} = \|\psi \wedge \phi\|^2 = 1 - |\langle \psi | \phi \rangle|^2$$

Thus, by Theorem 11,  $\|\psi \wedge \phi\| = \sqrt{1 - 2^{-k}}$ .  $\square$

### 3.3 Linear dependence of stabilizer states

We now characterize linearly-dependent triplets of stabilizer states and discuss properties of minimally-dependent sets. Such properties can help in exploring succinct representations of arbitrary pure states using linear combinations of stabilizer states.

**Corollary 7** (of Theorem 13). *Every linearly-dependent triplet  $\{|s_1\rangle, |s_2\rangle, |s_3\rangle\}$  of stabilizer states that are non-parallel to each other includes two pairs of nearest neighbors and one pair of orthogonal states. Furthermore, every nearest-neighbor pair gives rise to a triplet of linearly-dependent stabilizer states with two pairs of nearest neighbors and one pair of orthogonal states.*

**Proof.** Without loss of generality, assume that  $|s_1\rangle = \alpha|s_2\rangle + \beta|s_3\rangle$  and  $|s_1\rangle = |00\dots 0\rangle$ . Recall from Corollary 2 that the non-zero amplitudes of a stabilizer state  $|s\rangle$  are  $\pm 1/\sqrt{|s|}$  or  $\pm i/\sqrt{|s|}$  and its support  $|s|$  is a power of two. By our assumptions, the supports of  $|s_2\rangle$  and  $|s_3\rangle$  cannot differ by more than one.

*Case 1:*  $|s_2| \neq |s_3|$ . Then one of  $|s_2\rangle$  and  $|s_3\rangle$  has support one, while the other has support two. Suppose  $|s_2| = 2$ . By Lemma 2,  $|s_2\rangle = \frac{|00\dots 0\rangle + i^l|b\rangle}{\sqrt{2}}$ , where  $l \in \{0, 1, 2, 3\}$  and  $|b\rangle$  is computational-basis state other than  $|00\dots 0\rangle$ . Thus,  $|s_1\rangle$  and  $|s_2\rangle$  are nearest neighbors. Since  $|s_3| = 1$  and the triplet is linearly dependent,  $|s_3\rangle = \sqrt{2}|s_2\rangle - |s_1\rangle = i^l|b\rangle$ . Therefore,  $|s_3\rangle$  is orthogonal to  $|s_1\rangle$  and a nearest neighbor to  $|s_2\rangle$ .

*Case 2:*  $|s_2| = |s_3|$ . At least one of  $|s_2\rangle$  and  $|s_3\rangle$  must have a non-zero amplitude at  $|00\dots 0\rangle$ . If only one does, say  $|s_2\rangle$ , then  $|s_3\rangle$  will have a non-zero amplitude at some other basis state where  $|s_2\rangle$  has zero amplitude, preventing  $|s_1\rangle = \alpha|s_2\rangle + \beta|s_3\rangle$  from being  $|00\dots 0\rangle$ . Thus, both  $|s_2\rangle$  and  $|s_3\rangle$  must have a non-zero amplitude at  $|00\dots 0\rangle$  and, more generally, their non-zero amplitudes must all be at the same basis elements.

As non-zero amplitudes of stabilizer states must be either real or imaginary, we normalize the global phases of  $|s_2\rangle$  and  $|s_3\rangle$  so that the  $|00\dots 0\rangle$  amplitudes are real, which implies that  $\alpha$  and  $\beta$  are real. Using additional multiplication by  $\pm 1$ , we ensure that  $\alpha, \beta > 0$ . Considering the amplitudes at  $|00\dots 0\rangle$ , linear dependence implies  $\pm \frac{\alpha}{\sqrt{|s_2|}} \pm \frac{\beta}{\sqrt{|s_3|}} = 1$ . Furthermore,  $\alpha, \beta > 0$  and  $|s_2| = |s_3|$  leave three possibilities:  $\alpha \pm \beta = \sqrt{|s_2|}$  and  $\beta - \alpha = \sqrt{|s_2|}$ . At any other basis element where  $|s_2\rangle$  and  $|s_3\rangle$  have non-zero amplitudes, there is the additional constraint that  $\alpha = \beta$  since these amplitudes must cancel out while  $\alpha, \beta > 0$ . This eliminates two of the three possibilities above, implying  $\alpha = \frac{1}{\sqrt{|s_2|}}$ ,  $\beta = \frac{1}{\sqrt{|s_2|}}$  and  $|s_2| = |s_3| = 2$ . By Lemma 2,  $|s_2\rangle$  and  $|s_3\rangle$  are nearest neighbors of  $|s_1\rangle$  and  $\langle s_2|s_3\rangle = 0$ .  $\square$

**Minimally-dependent sets of stabilizer states.** Given  $k > 3$ , we now consider sets of  $k$  stabilizer states that are *linearly dependent*, but such that all of their proper subsets are *independent*. One such possibility are sets that contain  $k - 1$  mutually orthogonal stabilizer states and their sum. Consider the computational basis and a superposition of basis states that is also a stabilizer state. Theorem 9 and Corollary 2 suggest examples of such minimally-dependent sets with  $k = 2^m + 1$  stabilizer states. Suppose  $k = 2^m - d$  and  $|s\rangle$  is a stabilizer state in a superposition of all  $2^m$  computational-basis states. To construct a minimally-dependent set of size  $k$ , replace  $2d + 2$  basis states with  $d + 1$  stabilizer states formed as half-sums of  $d + 1$  disjoint pairs of basis states. Note that all stabilizer states except for  $|s\rangle$  remain orthogonal and contribute to  $|s\rangle$ .

**Example 21.** Let  $|s\rangle = \frac{1}{2\sqrt{2}} \sum_{i=0}^7 |b_i\rangle$  where each  $|b_i\rangle$  is a computational-basis state. One can obtain a minimally-dependent set of size  $k = 5$  as  $\{(|b_0\rangle + |b_1\rangle), (|b_2\rangle + |b_3\rangle), (|b_4\rangle + |b_5\rangle), (|b_6\rangle + |b_7\rangle), |s\rangle\}$ , where each state in parentheses is a half-sum of two basis states.

We close this section by outlining how to test the linear (in)dependence of a finite set of stabilizer states  $\mathbf{s} = \{|s_1\rangle, \dots, |s_k\rangle\}$ . Recall that the *Gramian* of  $\mathbf{s}$  is a matrix whose entries are given by  $\langle s_j | s_i \rangle$ , and that  $\mathbf{s}$  is linearly dependent if and only if the determinant of its Gramian matrix is zero. In Section 5.2, we describe an inner-product algorithm for stabilizer states. Thus, to test the linear (in)dependence of  $\mathbf{s}$ , generate the Gramian matrix by computing pairwise inner products using our algorithm.<sup>i</sup> Then, compute the determinant of the Gramian matrix and compare it to zero.

#### 4 The Embedding of Stabilizer Geometry in Hilbert Space

The geometric structure of stabilizer states described in Section 3.1 suggests an equally-spaced embedding in the finite-dimensional Hilbert space that can be exploited to study arbitrary quantum states. This is further evidenced by two types of results. First, the uniform distribution over stabilizer states is close to the uniform distribution of arbitrary

<sup>i</sup> The performance of pairwise computation of inner products between stabilizer states using techniques in Section 5.2 can be improved by pre-computing and storing a basis normalization circuit for each state, rather than computing it from scratch for each pair of states.

quantum states in terms of their first two moments [11, 24, 26]. Second, the entanglement of stabilizer states is nearly maximal and similar to that of random states [7, 31].

Consider a linear combination of stabilizer states  $\sum_{i=1}^k \alpha_i |s_i\rangle$  and the task of finding a closest stabilizer state:

$$\arg \max_{|\phi\rangle \in \text{Stab}(\mathcal{H})} |\sum_{i=1}^k \alpha_i \langle \phi | s_i \rangle| \quad (15)$$

where  $\text{Stab}(\mathcal{H})$  is the set of stabilizer states in the Hilbert space  $\mathcal{H}$ . Here, we can work with any representation of  $|\phi\rangle$  that allows us to compute inner products with stabilizer states, e.g., a succinct superposition of stabilizer states. The large count of nearest-neighbor stabilizer states given by Theorem 15 and the rather uniform structure of stabilizer geometry (Theorem 17, Corollary 5) motivate the use of local search to compute Formula 15. However, it turns out that greedy local search does not guarantee finding a closest stabilizer state.

#### 4.1 Approximating an arbitrary quantum state with a single stabilizer state

We analyze a simple *greedy local-search* algorithm that starts at the stabilizer state  $|s_m\rangle$  in  $|\psi\rangle = \sum_{i=1}^k \alpha_i |s_i\rangle$  with the largest  $|\alpha_i|$ . At each iteration, this algorithm evaluates the nearest neighbors  $N(|s_m\rangle)$  of the current state  $|s_m\rangle$  by computing  $\max_{|\phi\rangle \in N(|s_m\rangle)} |\langle \phi | \psi \rangle|$ , and then moves to a neighbor that satisfies this metric. The algorithm stops at a stabilizer state that is closer to  $|\psi\rangle$  than any of its nearest neighbors. As an illustration, consider the state

$$|\psi\rangle = (1 + \varepsilon) |00\rangle + |01\rangle + |10\rangle + |11\rangle \quad (16)$$

Given a sufficiently small  $\varepsilon > 0$ , the unique closest stabilizer state to  $|\psi\rangle$  is  $|00\rangle + |01\rangle + |10\rangle + |11\rangle$ . We start local search at  $|s_m\rangle = |00\rangle$  which contributes most to  $|\psi\rangle$ . By Theorem 13, all nearest neighbors of  $|00\rangle$  have the form  $\frac{|00\rangle + J|ab\rangle}{\sqrt{2}}$  where  $ab \in \{01, 10, 11\}$  and  $J \in \{\pm 1, \pm i\}$ . Here we maintain global constants, as they make a difference. We also pick a representative value  $ab = 01$  and note that the inner product with  $|\psi\rangle$  is maximized by  $J = 1$ . Let  $|r\rangle = (|00\rangle + |01\rangle)/\sqrt{2}$ . When  $\langle \psi | 00 \rangle = 1 + \varepsilon < \langle \psi | r \rangle = (2 + \varepsilon)/\sqrt{2}$  (up to the same constant), the algorithm sets  $|s_m\rangle = |r\rangle$ . Nearest neighbors of  $|s_m\rangle = \frac{|00\rangle + |01\rangle}{\sqrt{2}}$  are its half-sums with its orthogonal stabilizer states, hence we arrive at  $\frac{|00\rangle + |01\rangle + |10\rangle + |11\rangle}{2}$ . Consider the  $n$ -qubit state

$$|\psi_n\rangle = (1 + \varepsilon) |0 \dots 00\rangle + |0 \dots 01\rangle + \dots + |1 \dots 1\rangle \quad (17)$$

Its inner products with  $|0 \dots 00\rangle$  and the full-superposition state (up to the same constant) are  $(1 + \varepsilon)$  and  $(2^n + \varepsilon)/2^{n/2}$ , respectively. The full-superposition state will be closer as long as  $\varepsilon < \frac{2^n - 2^{n/2}}{2^{n/2} - 1} = 2^{n/2}$ . If we start local search at  $|0 \dots 0\rangle$ , it will terminate there when  $\varepsilon > \frac{2 - \sqrt{2}}{\sqrt{2} - 1} = \sqrt{2}$ , regardless of  $n$ . Thus, local search stops at a suboptimal stabilizer state when  $\sqrt{2} < \varepsilon < 2^{n/2}$ .

Even though constructive approximation by single stabilizer states appears difficult, it is important to know if good approximations exist. As we show next, the answer is negative for the more general case of approximating by stabilizer superpositions.

#### 4.2 Approximating arbitrary states with superpositions of stabilizer states

The geometric structure of stabilizer states also motivates the approximation of arbitrary  $n$ -qubit unbiased states using superpositions of  $\text{poly}(n)$  stabilizer states. In particular, some

optimism for obtaining quality approximations using *small* superpositions is motivated by the count of  $n$ -qubit stabilizer states from Equation 1 — the  $\Omega(2^{n^2/2})$  growth rate can be contrasted with the  $2^n$  growth rate of the number of basis states.

To evaluate the quality of approximation by stabilizer states, we employ the quantities

$$\Upsilon = \lim_{n \rightarrow \infty} \inf_{|\psi\rangle} \max_{|s\rangle \in \mathcal{S}_n} \langle s|\psi\rangle \quad \text{and} \quad \Upsilon^{\text{poly}} = \sup_{\text{poly}} \lim_{p(n)} \inf_{|\psi\rangle} \sup_{|s\rangle \in \mathcal{S}_n^{p(n)}} \langle s|\psi\rangle \quad (18)$$

where  $\mathcal{S}_n^{p(n)}$  contains superpositions of up to  $p(n)$  states from the set of all  $\mathcal{S}_n$  for a given polynomial  $p(n)$ . For illustration, replace  $\mathcal{S}_n$  with a set  $\mathcal{B}_n$  of  $2^n$  orthogonal basis states. The state  $|\psi\rangle = \frac{1}{2^{n/2}} \sum_{k=0}^{2^n-1} |k\rangle$  minimizes  $\max_{s \in \mathcal{B}_n} \langle s|\psi\rangle$  with the value  $\frac{1}{2^{n/2}}$ . Because this value approaches zero at an exponential rate, taking polynomial-sized superpositions of basis states (rather than single basis states) will still produce the zero limit. Perhaps, this result is not surprising given that  $\max_{|s_1\rangle \neq |s_2\rangle \in \mathcal{B}_n} \langle s_1|s_2\rangle = 0$ . However, since  $\max_{|s_1\rangle \neq |s_2\rangle \in \mathcal{S}_n} \langle s_1|s_2\rangle = 1/\sqrt{2}$ , and each stabilizer state  $|s_1\rangle \in \mathcal{S}_n$  has  $2^{n+2} - 4$  nearest neighbors  $|s_2\rangle \in \mathcal{S}_n$  such that  $\langle s_1|s_2\rangle = 1/\sqrt{2}$ , one might hope that  $\Upsilon = 1/\sqrt{2}$ .

**Lemma 4.** *Given an  $n$ -qubit stabilizer state  $|s\rangle$  and two qubits  $q$  and  $r$ , supports and norms of all non-zero double cofactors  $|s_{qr}\rangle$  are equal. In particular, since all supports are powers of two, the number of double cofactors with non-zero support cannot be three.*

**Proof.** The claim is trivial when only one double cofactor is non-zero. When only two are non-zero, they may originate from one single-qubit cofactor or from two different single-qubit cofactors. By Corollary 2-iv, the supports and norms of cofactors must be equal. When all four double cofactors are non-zero, Corollary 2-iv implies that their support must be one fourth of that of the initial state. Additionally, the orthogonality of cofactors implies that their norm must be one half of the original norm. Now we show that the case of exactly three non-zero double cofactors is impossible. Without the loss of generality, assume that  $|\psi_{qr=11}\rangle = 0$ , but other cofactors are  $\neq 0$ . Then single cofactors must have equal support. Therefore  $|\psi_{r=1}| = |\psi_{qr=01}| = |\psi_{qr=00}| + |\psi_{qr=10}| = |\psi_{r=0}| = 2|\psi_{qr=10}|$ , but also  $|\psi_{q=1}| = |\psi_{qr=10}| = |\psi_{qr=00}| + |\psi_{qr=01}| = |\psi_{q=0}| = 2|\psi_{qr=01}|$ . Thus  $|\psi_{qr=01}| = 4|\psi_{qr=01}|$ , which contradicts  $|\psi_{qr=01}| \neq 0$ .  $\square$

Lemma 4 is illustrated in Table 2 and Appendix A.

**Theorem 22.**  $\Upsilon = \Upsilon^{\text{poly}} = 0$ .

**Proof.** Consider the family of  $2n$ -qubit unbiased states  $\mu^{2n} = \left( \frac{|00\rangle + |01\rangle + |10\rangle}{\sqrt{3}} \right)^{\otimes n}$ , which are not stabilizer states per Lemma 4. For an arbitrary stabilizer state  $|s\rangle$ , double cofactoring over  $q = 2n - 1$  and  $r = 2n - 2$  yields

$$\langle s|\mu^{2n}\rangle = \langle s_{qr=00}|\mu_{qr=00}^{2n}\rangle + \langle s_{qr=01}|\mu_{qr=01}^{2n}\rangle + \langle s_{qr=10}|\mu_{qr=10}^{2n}\rangle \quad (19)$$

because  $|\mu_{qr=11}^{2n}\rangle = 0$ . We can upper-bound this expression by over-estimating each non-zero term with  $\langle v|w\rangle \leq \|v\| \cdot \|w\|$ . To this end,  $\|\mu_{qr}^{2n}\| = \frac{1}{\sqrt{3}}$ , while the norm of (orthogonal) double cofactors of  $|s\rangle$  depends on how many of them are non-zeros — one, two or four. In these cases, the norms are 1,  $\frac{\sqrt{2}}{2}$  and  $\frac{1}{2}$ , respectively, yielding upper bounds  $\langle s|\mu^{2n}\rangle \leq \alpha = \frac{\sqrt{3}}{3}, \frac{\sqrt{6}}{3}$  and  $\frac{\sqrt{3}}{2}$ . Therefore, cumulatively,  $\langle s|\mu^{2n}\rangle \leq \frac{\sqrt{3}}{2}$ .

More accurate bounds can be obtained by rewriting the same three terms using

$$\langle v|w\rangle = \|v\| \cdot \|w\| \frac{\langle v|w\rangle}{\|v\| \cdot \|w\|},$$

then observing that  $\langle v00|w00\rangle = \langle v|w\rangle$ ,  $\langle v01|w01\rangle = \langle v|w\rangle$ , and  $\langle v10|w10\rangle = \langle v|w\rangle$ . In particular,  $\sqrt{3}|\mu_{qr=00}^{2n}\rangle$ ,  $\sqrt{3}|\mu_{qr=01}^{2n}\rangle$  and  $\sqrt{3}|\mu_{qr=10}^{2n}\rangle$  can be replaced by  $|\mu^{2n-2}\rangle$ , noting that  $|\mu^{2n}\rangle$  is separable. Then the cofactors of  $|s\rangle$  can be relaxed to a best-case  $(2n-2)$ -qubit stabilizer state  $s'$  to obtain

$$\langle s|\mu^{2n}\rangle \leq \frac{\sqrt{3}}{2}\langle s'|\mu^{2n-2}\rangle \leq \left(\frac{\sqrt{3}}{2}\right)^n \quad (20)$$

Therefore

$$\Upsilon = \lim_{n \rightarrow \infty} \inf_{|\psi\rangle} \max_{|s\rangle \in \mathcal{S}_{2n}} \langle s|\psi\rangle = \lim_{n \rightarrow \infty} \left(\frac{\sqrt{3}}{2}\right)^n = 0 \quad (21)$$

For any polynomial  $p(n)$ ,

$$\lim_{n \rightarrow \infty} \inf_{|\psi\rangle} \sup_{|s\rangle \in \mathcal{S}_{2n}^{p(n)}} \langle s|\psi\rangle = \lim_{n \rightarrow \infty} p(n) \left(\frac{\sqrt{3}}{2}\right)^n = 0 \quad (22)$$

Therefore  $\Upsilon^{poly} = 0$  as well.  $\square$

Theorem 22 is somewhat surprising because no  $n$ -qubit state can be orthogonal to the set of all stabilizer states, which contains many basis sets. However, they establish *asymptotic orthogonality*, which can be viewed as an infinite-dimensional phenomenon. Such families of states that are asymptotically orthogonal to all stabilizer states can be neither represented nor approximated by polynomial-sized superpositions of stabilizer states.

Our construction of *stabilizer-evading* states can be modified to yield other *separable* states with similar properties, e.g.,  $\bar{\mu}^{3n} = \left(\frac{|001\rangle + |010\rangle + |100\rangle}{\sqrt{3}}\right)^{\otimes n}$ . Superpositions such as  $(\mu^{6n} + \bar{\mu}^{6n})/\sqrt{2}$  offer *entangled* states that cannot be approximated by polynomial-sized superpositions of stabilizer states.

The above results along with the results from Section 4.1 suggest that there are wide gaps between stabilizer states. The following proposition quantifies the size of such gaps.

**Proposition 23.** *Consider  $2^n$ -dimensional balls centered at a point on the unit sphere that do not contain any  $n$ -qubit stabilizer states in their interior. The radius of such balls cannot exceed  $\sqrt{2}$ , but approaches  $\sqrt{2}$  as  $n \rightarrow \infty$ .*

**Proof sketch.** Consider an arbitrary ball  $\mathbf{B}$  with radius  $\sqrt{2}$  and centered on the unit sphere as shown in Figure 6.  $\mathbf{B}$  covers half of the unit sphere. Let  $|s\rangle$  be a stabilizer state that does not lie on the boundary of  $\mathbf{B}$ . Then, either  $|s\rangle$  or  $-|s\rangle$  is inside  $\mathbf{B}$ . Furthermore, observe that the intersection of the unit sphere and the boundary of  $B$  is contained in a hyperplane of dimension  $n-1$ . If all stabilizer states were contained there, they would not have included a single basis set. However, since stabilizer states contain the computational basis, they cannot all be contained in that intersection. An asymptotic lower bound for the radius of  $B$  is obtained using the family of *stabilizer-evading* states defined in Theorem 22. These states are asymptotically orthogonal to all  $n$ -qubit stabilizer states ( $n \rightarrow \infty$ ). Therefore, the distance to their closest stabilizer state approaches  $\sqrt{2}$ .  $\square$

## 5 Computational Geometry of Stabilizer States

Section 4 illustrates how straightforward approaches to several natural geometric tasks fail. In this section, we focus on more specialized, but no less useful tasks and develop computational techniques that we successfully implemented in software and evaluate in Section 6.

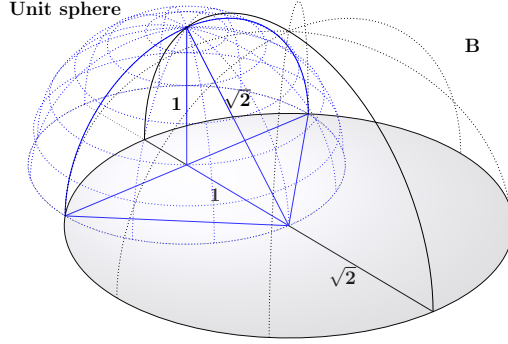


Fig. 6. A ball  $\mathbf{B}$  with radius  $\sqrt{2}$  centered on the unit sphere covers half of the unit sphere. Every such ball contains at least one stabilizer state (in most cases, half of all stabilizer states).

In Section 5.1, we discuss our algorithm for synthesizing new *canonical stabilizer circuits*. In Section 5.2, we turn our attention to the computation of inner products of stabilizer states and, by extension, their linear combinations. As Gram-Schmidt orthogonalization cannot be used directly with stabilizer states, we develop an alternative approach in Section 5.3. The efficient computation of generator sets for stabilizer bivectors is discussed in Section 5.4.

### 5.1 *Synthesis of canonical stabilizer circuits*

A crucial step in the inner-product computation for stabilizer states (Theorem 11) is the synthesis of a stabilizer circuit that brings an  $n$ -qubit stabilizer state  $|\psi\rangle$  to a computational basis state  $|b\rangle$ . Consider a stabilizer matrix  $\mathcal{M}$  that uniquely identifies  $|\psi\rangle$ .  $\mathcal{M}$  is reduced to basis form (Definition 2) by applying a series of elementary row and column operations. Recall that row operations (transposition and multiplication) do not modify the state, but column (Clifford) operations do. Thus, the column operations involved in the reduction process constitute a unitary stabilizer circuit  $\mathcal{C}$  such that  $\mathcal{C}|\psi\rangle = |b\rangle$ , where  $|b\rangle$  is a basis state. Algorithm 5.1 reduces an input matrix  $\mathcal{M}$  to basis form and returns such a circuit  $\mathcal{C}$ .

**Definition 7.** Given a finite sequence of quantum gates, a *circuit template* describes a segmentation of the circuit into blocks where each block uses only one gate type. The blocks must match the sequence and be concatenated in that order. For example, a circuit satisfying the  $H$ - $C$ - $P$  template starts with a block of Hadamard ( $H$ ) gates, followed by a block of CNOT ( $C$ ) gates, followed by a block of Phase ( $P$ ) gates.

**Definition 8.** A circuit with a *template structure* consisting entirely of stabilizer-gate blocks is called a *canonical stabilizer circuit*.

Canonical forms are useful for synthesizing stabilizer circuits that minimize the number of gates and qubits required to produce a particular computation. This is particularly important in the context of quantum fault-tolerant architectures that are based on stabilizer codes. The work in [2] establishes a 7-block<sup>j</sup> canonical-circuit template with the sequence  $H$ - $C$ - $P$ - $C$ - $P$ - $C$ - $H$ . Furthermore, the work in [32] proves the existence of canonical circuits with the shorter sequence  $H$ - $C$ - $X$ - $P$ - $CZ$ , where the  $X$  and  $CZ$  blocks consist of NOT and Controlled- $Z$  (CPHASE) gates, respectively. However, the synthesis algorithm sketched in [32] employs

<sup>j</sup>Theorem 8 in [2] actually describes an 11-step procedure to obtain such circuits. However, the last four steps are used to reduce destabilizer rows, which we do not consider here.



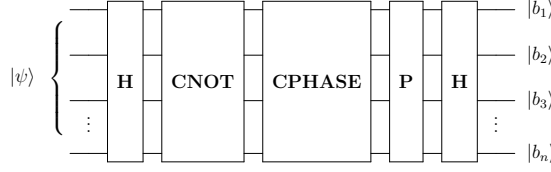


Fig. 7. Template structure for the basis-normalization circuit synthesized by Algorithm 5.1. The input is an arbitrary stabilizer state  $|\psi\rangle$  while the output is a basis state  $|b_1 b_2 \dots b_n \in \{0, 1\}^n\rangle$ .

the  $\mathbb{Z}_2$ -representation for states (Theorem 9) rather than the stabilizer formalism. Thus, no detailed algorithms are known for obtaining such canonical circuits *given an arbitrary generator set*. Algorithm 5.1 takes as input a stabilizer matrix  $\mathcal{M}$  and synthesizes a 5-block canonical circuit with template  $H-C-CZ-P-H$  (Figure 7). We now describe the main steps in the algorithm. The updates to the phase vector under row/column operations are left out of the discussion as such updates do not affect the overall execution of the algorithm.

1. Reduce  $\mathcal{M}$  to canonical form.
2. Use row transposition to diagonalize  $\mathcal{M}$ . For  $j \in \{1, \dots, n\}$ , if the diagonal literal  $\mathcal{M}_{j,j} = Z$  and there are other Pauli (non- $I$ ) literals in the row (qubit is entangled), conjugate  $\mathcal{M}$  by  $H_j$ . Elements below the diagonal are  $Z/I$  literals.
3. For each above-diagonal element  $\mathcal{M}_{j,k} = X/Y$ , conjugate by  $\text{CNOT}_{j,k}$ . Elements above the diagonal are now  $I/Z$  literals.
4. For each above-diagonal element  $\mathcal{M}_{j,k} = Z$ , conjugate by  $\text{CPHASE}_{j,k}$ . Elements above the diagonal are now  $I$  literals.
5. For each diagonal literal  $\mathcal{M}_{j,j} = Y$ , conjugate by  $P_j$ .
6. For each diagonal literal  $\mathcal{M}_{j,j} = X$ , conjugate by  $H_j$ .

**Proposition 24.** *For an  $n \times n$  stabilizer matrix  $\mathcal{M}$ , the number of gates in the circuit  $\mathcal{C}$  returned by Algorithm 5.1 is  $O(n^2)$ .*

**Proof.** The number of gates in  $\mathcal{C}$  is dominated by the CPHASE block, which consists of  $O(n^2)$  gates. This agrees with previous results regarding the number of gates needed for an  $n$ -qubit stabilizer circuit in the worst case [6, 10].  $\square$

Observe that, for each gate added to  $\mathcal{C}$ , the corresponding column operation is applied to  $\mathcal{M}$ . Since column operations run in  $\Theta(n)$  time, it follows from Proposition 29 that the runtime of Algorithm 5.1 is  $O(n^3)$ . Audenaert and Plenio [4] described an algorithm to compute the fidelity between two mixed stabilizer states. Similar to our use of basis-normalizing circuits, the approach from [4] relies on a stabilizer circuit to map a stabilizer state to a normal form where all basis states have non-zero amplitudes. However, the circuits generated by the Audenaert-Plenio algorithm exhibit two disadvantages: (i) they are not canonical and (ii) they have, on average, twice as many gates as our basis-normalization circuits (Section 6).

We note that our canonical stabilizer circuits can be optimized using the techniques from [27], which describes how to restructure circuits to facilitate parallel quantum computation. The authors show that such parallelization is possible for circuits consisting of  $H$  and  $\text{CNOT}$  gates, and for diagonal operators. Since CPHASE gates are diagonal, one can apply the techniques from [27] to parallelize our canonical circuits and produce equivalent circuits with  $O(n^2)$  gates and parallel depth  $O(\log n)$ . Canonical stabilizer circuits that follow

**Algorithm 5.1** Synthesis of a basis-normalization circuit**Input:** Stabilizer matrix  $\mathcal{M}$  for  $S(|\psi\rangle)$  with rows  $R_1, \dots, R_n$ **Output:** (i) Unitary stabilizer circuit  $\mathcal{C}$  such that  $\mathcal{C}|\psi\rangle$  equals basis state  $|b\rangle$ , and (ii) reduce  $\mathcal{M}$  to basis form  
 $\Rightarrow$  GAUSS( $\mathcal{M}$ ) reduces  $\mathcal{M}$  to canonical form (Figure 3) $\Rightarrow$  ROWSWAP( $\mathcal{M}, i, j$ ) swaps rows  $R_i$  and  $R_j$  of  $\mathcal{M}$  $\Rightarrow$  ROWMULT( $\mathcal{M}, i, j$ ) left-multiplies rows  $R_i$  and  $R_j$ , returns updated  $R_i$  $\Rightarrow$  CONJ( $\mathcal{M}, \alpha_j$ ) conjugates  $j^{th}$  column of  $\mathcal{M}$  by Clifford sequence  $\alpha$ 


---

```

1: GAUSS( $\mathcal{M}$ ) ▷ Set  $\mathcal{M}$  to canonical form
2:  $\mathcal{C} \leftarrow \emptyset$ 
3: for  $j \in \{1, \dots, n\}$  do ▷ Apply block of Hadamard gates
4:    $k \leftarrow$  index of row  $R_{k \in \{j, \dots, n\}}$  with  $j^{th}$  literal set to  $X$  or  $Y$ 
5:   if  $k$  exists then
6:     ROWSWAP( $\mathcal{M}, j, k$ )
7:   else
8:      $k_2 \leftarrow$  index of last row  $R_{k_2 \in \{j, \dots, n\}}$  with  $j^{th}$  literal set to  $Z$ 
9:     if  $k_2$  exists then
10:      ROWSWAP( $\mathcal{M}, j, k_2$ )
11:      if  $R_j$  has  $X, Y$  or  $Z$  literals in columns  $\{j+1, \dots, n\}$  then
12:        CONJ( $\mathcal{M}, H_j$ )
13:         $\mathcal{C} \leftarrow \mathcal{C} \cup H_j$ 
14:      end if
15:    end if
16:  end if
17: end for
18: for  $j \in \{1, \dots, n\}$  do ▷ Apply block of CNOT gates
19:   for  $k \in \{j+1, \dots, n\}$  do
20:     if  $k^{th}$  literal of row  $R_j$  is set to  $X$  or  $Y$  then
21:       CONJ( $\mathcal{M}, \text{CNOT}_{j,k}$ )
22:        $\mathcal{C} \leftarrow \mathcal{C} \cup \text{CNOT}_{j,k}$ 
23:     end if
24:   end for
25: end for
26: for  $j \in \{1, \dots, n\}$  do ▷ Apply a block of Controlled- $Z$  gates
27:   for  $k \in \{j+1, \dots, n\}$  do
28:     if  $k^{th}$  literal of row  $R_j$  is set to  $Z$  then
29:       CONJ( $\mathcal{M}, \text{CPHASE}_{j,k}$ )
30:        $\mathcal{C} \leftarrow \mathcal{C} \cup \text{CPHASE}_{j,k}$ 
31:     end if
32:   end for
33: end for
34: for  $j \in \{1, \dots, n\}$  do ▷ Apply block of Phase gates
35:   if  $j^{th}$  literal of row  $R_j$  is set to  $Y$  then
36:     CONJ( $\mathcal{M}, P_j$ )
37:      $\mathcal{C} \leftarrow \mathcal{C} \cup P_j$ 
38:   end if
39: end for
40: for  $j \in \{1, \dots, n\}$  do ▷ Apply block of Hadamard gates
41:   if  $j^{th}$  literal of row  $R_j$  is set to  $X$  then
42:     CONJ( $\mathcal{M}, H_j$ )
43:      $\mathcal{C} \leftarrow \mathcal{C} \cup H_j$ 
44:   end if
45: end for
46: return  $\mathcal{C}$ 

```

---

the 7-block template structure from [2] can be optimized to obtain a tighter bound on the number of gates. As in our approach, such circuits are dominated by the size of the CNOT blocks, which contain  $O(n^2)$  gates. The work in [29] shows that any CNOT circuit has an

**Algorithm 5.2** Inner product for stabilizer states

---

**Input:** Stabilizer matrices (i)  $\mathcal{M}^\psi$  for  $|\psi\rangle$  with rows  $P_1, \dots, P_n$ , and (ii)  $\mathcal{M}^\phi$  for  $|\phi\rangle$  with rows  $Q_1, \dots, Q_n$   
**Output:** Inner product between  $|\psi\rangle$  and  $|\phi\rangle$   
 $\Rightarrow$  BASISNORMCIRC( $\mathcal{M}^\psi$ ) reduces  $\mathcal{M}$  to basis form, i.e.  $\mathcal{C}|\psi\rangle = |b\rangle$ , where  $|b\rangle$  is a basis state, and returns  $\mathcal{C}$   
 $\Rightarrow$  CONJ( $\mathcal{M}, \mathcal{C}$ ) conjugates  $\mathcal{M}$  by Clifford circuit  $\mathcal{C}$   
 $\Rightarrow$  GAUSS( $\mathcal{M}$ ) reduces  $\mathcal{M}$  to canonical form (Figure 3)  
 $\Rightarrow$  LEFTMULT( $P, Q$ ) left-multiplies Pauli operators  $P$  and  $Q$ , and returns the updated  $Q$

---

```

1:  $\mathcal{C} \leftarrow \text{BASISNORMCIRC}(\mathcal{M}^\psi)$                                  $\triangleright$  Apply Algorithm 5.1 to  $\mathcal{M}^\psi$ 
2:  $\text{CONJ}(\mathcal{M}^\phi, \mathcal{C})$                                                $\triangleright$  Compute  $\mathcal{C}|\phi\rangle$ 
3:  $\text{GAUSS}(\mathcal{M}^\phi)$                                                $\triangleright$  Set  $\mathcal{M}^\phi$  to canonical form
4:  $k \leftarrow 0$ 
5: for each row  $Q_i \in \mathcal{M}^\phi$  do
6:   if  $Q_i$  contains  $X$  or  $Y$  literals then
7:      $k \leftarrow k + 1$ 
8:   else                                                          $\triangleright$  Check orthogonality, i.e.,  $Q_i \notin S(|b\rangle)$ 
9:      $R \leftarrow I^{\otimes n}$ 
10:    for each  $Z$  literal in  $Q_i$  found at position  $j$  do
11:       $R \leftarrow \text{LEFTMULT}(P_j, R)$ 
12:    end for
13:    if  $R = -Q_i$  then
14:      return 0                                                     $\triangleright$  By Theorem 10
15:    end if
16:  end if
17: end for
18: return  $2^{-k/2}$                                                $\triangleright$  By Theorem 11

```

---

equivalent CNOT circuit with  $O(n^2/\log n)$  gates. Thus, one simply applies such techniques to each of the CNOT blocks in the canonical circuit. It is an open problem whether one can apply some variation of the same techniques to CPHASE blocks, which would facilitate similar optimizations for our 5-block canonical form.

**5.2 An inner-product algorithm**

Let  $|\psi\rangle$  and  $|\phi\rangle$  be two stabilizer states represented by stabilizer matrices  $\mathcal{M}^\psi$  and  $\mathcal{M}^\phi$ , respectively. Our approach for computing the inner product between these two states is shown in Algorithm 5.2. Following the proof of Theorem 11, Algorithm 5.1 is applied to  $\mathcal{M}^\psi$  in order to reduce it to basis form. The stabilizer circuit generated by Algorithm 5.1 is then applied to  $\mathcal{M}^\phi$  in order to preserve the inner product. Then, we minimize the number of  $X$  and  $Y$  literals in  $\mathcal{M}^\phi$  by applying Algorithm 2.1. Lastly, each generator in  $\mathcal{M}^\phi$  that anticommutes with  $\mathcal{M}^\psi$  (since  $\mathcal{M}^\psi$  is in basis form, we only need to check which generators in  $\mathcal{M}^\phi$  have  $X$  or  $Y$  literals) contributes a factor of  $1/\sqrt{2}$  to the inner product. If a generator in  $\mathcal{M}^\phi$ , say  $Q_i$ , commutes with  $\mathcal{M}^\psi$ , then we check orthogonality by determining whether  $Q_i$  is in the stabilizer group generated by  $\mathcal{M}^\psi$ . This is accomplished by multiplying the appropriate generators in  $\mathcal{M}^\psi$  such that we create Pauli operator  $R$ , which has the same literals as  $Q_i$ , and check whether  $R$  has an opposite sign to  $Q_i$ . If this is the case, then, by Theorem 10, the states are orthogonal. The bottleneck of Algorithm 5.2 is the call to Algorithm 5.1, and the overall runtime is  $O(n^3)$ . As Section 6 shows, the performance of our algorithm is sensitive to the input stabilizer matrix and takes  $O(n^2)$  time in important cases.

**Complex-valued inner product.** Recall that Algorithm 5.2 computes the *real-valued* (phase-normalized) inner product  $r = e^{-i\theta} \langle \psi | \phi \rangle$ . To compute the *complex-valued* inner prod-

uct, one needs to additionally calculate  $e^{-i\theta}$ . This is accomplished by modifying Algorithm 5.2 such that it maintains the global phases generated when computing  $\mathcal{C}|\psi\rangle$  and  $\mathcal{C}|\phi\rangle$ , where  $\mathcal{C}$  is the basis-normalization circuit from Algorithm 5.1. Let  $\alpha$  and  $\beta$  be the global phases of  $\mathcal{C}|\psi\rangle$  and  $\mathcal{C}|\phi\rangle$ , respectively. The complex-valued inner product is computed as  $\alpha^* \cdot \beta \cdot 2^{-k/2}$ . Since stabilizer matrices represent states up to a global phase (i.e., states are normalized such that the first non-zero basis amplitude is 1.0), the functions `BASISNORMCIRC`( $\mathcal{M}$ ) and `CONJ`( $\mathcal{M}, \mathcal{C}$ ) need to be modified to keep track of the global-phase factors generated when each gate in  $\mathcal{C}$  is applied to the input state. Let  $U$  be a stabilizer gate applied to the state  $|\psi\rangle$  represented by stabilizer matrix  $\mathcal{M}$ . The following process computes the global phase of  $U|\psi\rangle$ :

1. Use Gaussian elimination to obtain a basis state  $|b\rangle$  from  $\mathcal{M}$  (Observation 4) and store its non-zero amplitude  $\alpha$ . If  $U$  is the Hadamard gate, it may be necessary to sample a sum of two non-zero (one real, one imaginary) basis amplitudes (see Example 25).
2. Compute  $\alpha U|b\rangle = \alpha' |b'\rangle$  directly using the state-vector representation.
3. Obtain  $|b'\rangle$  from  $U\mathcal{M}U^\dagger$  and store its non-zero amplitude  $\beta$ .
4. The phase factor generated is  $\alpha'/\beta$ .

**Example 25.** Suppose  $|\psi\rangle = |00\rangle + |01\rangle - i|10\rangle - i|11\rangle$ , where we omit the normalization factor for clarity. A generator set for  $|\psi\rangle$  is  $\mathcal{M} = \{-YI, IX\}$ . We will compute the global-phase factor generated when a Hadamard gate is applied to the first qubit. Following Step 1, we obtain basis states  $|00\rangle$  and  $i|10\rangle$  from  $\mathcal{M}$ , and set  $\alpha = 1$  (the amplitude of  $|00\rangle$ ). Next, we compute  $H_1(|00\rangle + i|10\rangle) = \frac{1-i}{\sqrt{2}}|00\rangle + \frac{1+i}{\sqrt{2}}|10\rangle$  and set  $\alpha' = \frac{1-i}{\sqrt{2}}$  (Step 2). According to Step 3, we obtain the  $|00\rangle$  amplitude from  $H_1\mathcal{M}H_1^\dagger = \{YI, IX\}$ , which gives  $\beta = 1$ . The global-phase factor is  $\alpha'/\beta = \frac{1-i}{\sqrt{2}}$ . One can obtain the factor generated when CNOT, Phase and measurements gates are applied in a similar fashion. However, for such gates, only one basis-state amplitude needs to be sampled in Step 1.

### 5.3 Orthogonalization of stabilizer states

We now shift our focus to the task of orthogonalizing a linear combination of stabilizer states  $|\Psi\rangle = \sum_{j=1}^N c_j |\psi_j\rangle$ , where each  $|\psi_j\rangle$  is represented by its own stabilizer matrix. To simulate measurements of  $|\Psi\rangle$ , it is helpful to transform the set of states that define  $|\Psi\rangle$  into an orthogonal set. Since a linear combination of stabilizer states is usually not a stabilizer state, Gram-Schmidt orthogonalization cannot be used directly. Therefore, we develop an orthogonalization procedure that exploits the nearest-neighbor structure of stabilizer states (Section 3.1) and their efficient manipulation via stabilizers.

**Proposition 26.** *Let  $|\psi\rangle$  be a state represented by  $\mathcal{M}^\psi$ , which contains at least one row with at least one  $X$  or  $Y$  literal. Then  $|\psi\rangle$  can be decomposed into a superposition  $\frac{|\phi\rangle + i^l |\varphi\rangle}{\sqrt{2}}$ , where  $|\phi\rangle$  and  $|\varphi\rangle$  are nearest neighbors of  $|\psi\rangle$  whose matrices are similar to each other.*

**Proof.** Let  $R_j$  be a row in  $\mathcal{M}^\psi$  with an  $X/Y$  literal in its  $j^{\text{th}}$  position, and let  $Z_j$  be a Pauli operator with a  $Z$  literal in its  $j^{\text{th}}$  position and  $I$  everywhere else. Observe that  $R_j$  and  $Z_j$  anticommute. If any other rows in  $\mathcal{M}^\psi$  anticommute with  $Z_j$ , multiply them by  $R_j$  to make them commute with  $Z_j$ . Let  $\mathcal{M}^\phi$  and  $\mathcal{M}^\varphi$  be the matrices obtained by replacing row  $R_j$  in  $\mathcal{M}^\psi$  with  $Z_j$  and  $-Z_j$ , respectively. This operation is equivalent to applying  $(\pm Z_j)$ -measurement projectors to  $|\psi\rangle$ . Thus,  $|\phi\rangle \equiv \frac{(I+Z_j)|\psi\rangle}{\sqrt{2}}$  and  $|\varphi\rangle \equiv \frac{(I-Z_j)|\psi\rangle}{\sqrt{2}}$ , such that  $|\langle\psi|\phi\rangle| = |\langle\psi|\varphi\rangle| = 1/\sqrt{2}$ . The matrices  $\mathcal{M}^\phi$  and  $\mathcal{M}^\varphi$  are similar since  $\mathcal{M}^\varphi = X_j(\mathcal{M}^\phi)X_j^\dagger$

(and  $\mathcal{M}^\phi = X_j(\mathcal{M}^\varphi)X_j^\dagger$ ), where  $X_j$  is a Pauli operator with an  $X$  literal in its  $j^{\text{th}}$  position and  $I$  everywhere else. This implies that the  $j^{\text{th}}$  qubit in  $|\phi\rangle$  and  $|\varphi\rangle$  is in the deterministic state  $|0\rangle$  and  $|1\rangle$ , respectively. ( $|\phi\rangle$  and  $|\varphi\rangle$  are cofactors of  $|\psi\rangle$  with respect to qubit  $j$ .) To produce  $\frac{|\phi\rangle + i^l |\varphi\rangle}{\sqrt{2}}$ , we need the  $i^l$  factor, which is not maintained by the stabilizer  $\mathcal{M}^\varphi$ . This factor can be obtained by the same global-phase computation procedure described in Section 5.2 in the context of complex-valued inner products.  $\square$

Algorithm 5.3 takes as input a linear combination of  $n$ -qubit states  $|\Psi\rangle$  represented by a pair consisting of: (i) a list of *canonical stabilizer matrices*  $\mathbf{M} = \{\mathcal{M}^1, \dots, \mathcal{M}^N\}$  and (ii) a list of coefficients  $\mathbf{C} = \{c_1, \dots, c_N\}$ . The algorithm iteratively applies the decomposition procedure described in the proof of Proposition 26 until all the matrices in  $\mathbf{M}$  are *similar* (Definition 1) to each other. At each iteration, the algorithm selects a pivot qubit based on the composition of Pauli literals in the corresponding column. The states in the linear combination are decomposed with respect to the pivot only if there exists a pair of matrices in  $\mathbf{M}$  that contain different types of Pauli literals in the pivot column. Since similar matrices contain distinct phase vectors, the states represented by the modified list of matrices are mutually orthogonal (Theorem 10). The algorithm maintains the invariant that the sum of stabilizer states (represented by the pair  $\mathbf{M}$  and  $\mathbf{C}$ ) equals the (non-stabilizer) vector  $|\Psi\rangle$ . Observe that, for each pivot qubit that satisfies  $b = 1$ , the size of  $\mathbf{M}$  doubles. Let  $m$  be the maximum value in  $\{m_1, \dots, m_N\}$ , where  $m_j$  is the number of rows with  $X/Y$  literals in matrix  $\mathcal{M}^j$ . An orthogonalization approach that obtains  $|\Psi\rangle$  in the computational basis (i.e., calculating computational-basis amplitudes of each  $|\psi_j\rangle$  and summing them with weights  $c_j$ ) requires exactly  $2^m$  terms. In contrast, Algorithm 5.3 expands  $\mathbf{M}$  to  $2^k$  terms, where  $k \leq m$ . In particular, if the matrices in  $\mathbf{M}$  are “close” to similar (Definition 1), then  $k < m$  and thus Algorithm 5.3 provides an advantage over direct computation of basis amplitudes.

**Example 27.** Let  $\mathbf{M} = \{\mathcal{M}^1, \mathcal{M}^2\}$ , where  $\mathcal{M}^1$  and  $\mathcal{M}^2$  are  $n$ -qubit matrices. Suppose  $\mathcal{M}^1$  has  $X$  literals along its diagonal and  $I$  literals everywhere else. Similarly, assume  $\mathcal{M}^2$  follows the same diagonal structure, but replaces an  $X$  at diagonal position  $p$  with  $Y$ . Algorithm 5.3 decomposes both matrices over the selected pivot qubit  $p$  using Proposition 26, which yields a list of two similar matrices. In contrast, calculating the basis amplitudes of the states represented by  $\mathcal{M}^1$  and  $\mathcal{M}^2$  would require summing over  $2^n$  terms.

#### 5.4 Computation of stabilizer bivectors

In Section 3.2, we defined the notion of a *stabilizer bivector*, which can be used to represent antisymmetric basis states [20] compactly on conventional computers. We now describe an algorithm to efficiently compute a generator set for stabilizer bivectors.

Let  $|\psi\rangle$  and  $|\phi\rangle$  be two stabilizer states represented by matrices  $\mathcal{M}^\psi$  and  $\mathcal{M}^\phi$ , respectively. Algorithm 5.4 shows our approach to computing the stabilizer bivector  $|\psi \wedge \phi\rangle$ . First, we compute  $\langle \psi | \phi \rangle$  and obtain the canonical matrices for  $\mathcal{M}^\psi$  and  $\mathcal{M}^\phi$ . This allows us to determine whether the conditions established by the proof of Theorem 19 are satisfied. In the case that  $|\psi\rangle$  and  $|\phi\rangle$  are 1-neighbors, we modify the *dissimilar* matrices as per the proof of Theorem 19. This ensures that the input matrices are *similar* before computing the matrices for the tensor products  $|\psi \otimes \phi\rangle$  and  $|\phi \otimes \psi\rangle$ .

**Example 28.** Suppose  $\mathcal{M}^\psi = \{ZI, IZ\}$  and  $\mathcal{M}^\phi = \{XI, IZ\}$ , which represent a nearest-neighbor pair. Following Equation 13, we replace  $\mathcal{M}^\phi$  with  $X_1 \mathcal{M}^\psi X_1^\dagger = \{-ZI, IZ\}$  (or  $\mathcal{M}^\psi$

**Algorithm 5.3** Orthogonalization procedure for a linear combination of stabilizer states

---

**Input:** Linear combination of  $n$ -qubit states  $|\Psi\rangle = \sum_{j=1}^N c_j |\psi_j\rangle$  represented by (i) a list of *canonical stabilizer matrices*  $\mathbf{M} = \{\mathcal{M}^1, \dots, \mathcal{M}^N\}$  and (ii) a list of coefficients  $\mathbf{C} = \{c_1, \dots, c_N\}$

**Output:** Modified lists  $\mathbf{M}'$  and  $\mathbf{C}'$  representing a linear combination of *mutually orthogonal states*

$\Rightarrow$  PAULI( $\mathcal{M}, j$ ) returns 0 if the  $j^{\text{th}}$  column in  $\mathcal{M}$  has  $Z$  literals only (ignores  $I$  literals), 1 if it has  $X$  literals only, 2 if it has  $Y$  literals only, 3 if it has  $X/Z$  literals only, and 4 if it has  $Y/Z$  literals only

$\Rightarrow$  REMOVE( $\mathbf{M}, \mathbf{C}, j$ ) removes the  $j^{\text{th}}$  element in  $\mathbf{M}$  and  $\mathbf{C}$

$\Rightarrow$  INSERT( $\mathbf{M}, \mathbf{C}, \mathcal{M}, c$ ) appends  $\mathcal{M}$  to  $\mathbf{M}$  and  $c$  to  $\mathbf{C}$  if an *equivalent matrix* does not exist in  $\mathbf{M}$ ; otherwise, sets  $c_j = c_j + c$ , where  $c_j$  is the coefficient of the matrix in  $\mathbf{M}$  that is equivalent to  $\mathcal{M}$

$\Rightarrow$  DECOMPOSE( $\mathcal{M}, j, a \in \{0, 1\}$ ) implements the proof of Proposition 26 and returns the pair  $[\mathcal{M}_{j=a}, \alpha]$ , where  $\mathcal{M}_{j=a}$  is the nearest-neighbor canonical matrix with the  $j^{\text{th}}$  qubit in state  $|a\rangle$ , and  $\alpha$  is the phase factor

---

```

1: for  $j \in \{1, \dots, n\}$  do
2:    $b \leftarrow 0$ 
3:    $l \leftarrow \text{PAULI}(\mathcal{M}^1, j)$ 
4:   for each  $\mathcal{M}^i, i \in \{2, \dots, N\}$  do
5:      $k \leftarrow \text{PAULI}(\mathcal{M}^i, j)$ 
6:     if  $k \neq l$  or the rows with Pauli literals in the  $j^{\text{th}}$  column are distinct then
7:        $b \leftarrow 1$ 
8:       break
9:     end if
10:  end for
11:  if  $b = 1$  then
12:    for each  $\mathcal{M}^i, i \in \{1, \dots, N\}$  do
13:      if  $\text{PAULI}(\mathcal{M}^i, j) \neq 0$  then
14:         $[\mathcal{M}_{j=0}^i, \alpha] \leftarrow \text{DECOMPOSE}(\mathcal{M}^i, j, 0)$ 
15:         $[\mathcal{M}_{j=1}^i, \beta] \leftarrow \text{DECOMPOSE}(\mathcal{M}^i, j, 1)$ 
16:        REMOVE( $\mathbf{M}, \mathbf{C}, i$ )
17:        INSERT( $\mathbf{M}, \mathbf{C}, \mathcal{M}_{j=0}^i, \alpha/\sqrt{2}$ )
18:        INSERT( $\mathbf{M}, \mathbf{C}, \mathcal{M}_{j=1}^i, \beta/\sqrt{2}$ )
19:      end if
20:    end for
21:  end if
22: end for

```

---

with  $X_1 \mathcal{M}^\phi X_1^\dagger = \{-XI, IZ\}$ ) to make the input matrices similar.

The last step is to compute the difference  $|\psi \otimes \phi\rangle - |\phi \otimes \psi\rangle$  as follows:

1. Obtain the basis-normalization circuit  $\mathcal{C}$  for both  $\mathcal{M}^{\psi \otimes \phi}$  and  $\mathcal{M}^{\phi \otimes \psi}$ . Observe that its the same circuit since the matrices are similar.
2. Conjugate both matrices by  $\mathcal{C}$  to obtain the matrices for basis states  $|b_1\rangle$  and  $|b_2\rangle$ .
3. Following the proof of Lemma 2, obtain the matrix  $\mathcal{M}^{b_1-b_2}$  for the sum  $|b_1\rangle - |b_2\rangle$ .
4. Conjugate  $\mathcal{M}^{b_1-b_2}$  by  $\mathcal{C}^\dagger$  to obtain the matrix  $\mathcal{M}^{\psi \wedge \phi}$ .

**Proposition 29.** Let  $|\psi\rangle$  and  $|\phi\rangle$  be two  $n$ -qubit stabilizer states. The  $2n$ -qubit stabilizer bivector  $|\psi \wedge \phi\rangle$  can be computed in  $O(n^3)$  time.

**Proof.** The bottleneck in Algorithm 5.4 is the computation of the basis-normalization circuit for the  $2n \times 2n$  stabilizer matrix  $\mathcal{M}^{\psi \otimes \phi}$ , which takes  $O(n^3)$  time.  $\square$

### 5.5 Mixed stabilizer states

The work in [2] describes *mixed stabilizer states*, which are states that are *uniformly distributed* over all states in a subspace. Since such mixed states can be written as the partial trace of a pure stabilizer state, they can be represented compactly using stabilizer matrices. Recall from Theorem 1 that the set of Pauli operators (rows) in a stabilizer matrix that represents a pure state are linearly independent. In contrast, to represent mixed stabilizer states, one needs to maintain stabilizer matrices with linearly-dependent rows [2, 4]. This implies that a subset of the rows in the matrix can be reduced to the identity operator. Since Algorithm 2.1 reduces a stabilizer matrix to its Gauss-Jordan form, it can be used to find and eliminate linearly-dependent rows. Such rows will show up as  $I$ -literal only rows at the bottom of the matrix after Algorithm 2.1 is applied. Similarly, Algorithms 5.1 and 5.2, generalize to the case of mixed stabilizer states since one can identify linearly-dependent rows via Algorithm 2.1 and then ignore them throughout the rest of the computation. Therefore, if the input matrices represent mixed states, Algorithm 5.2 computes the fidelity between them.

As outlined in [2] and proven in [4], one can also compute the partial trace over qubit  $j$  as follows: (i) apply a modified version of Algorithm 2.1 such that the  $j^{th}$  column of the stabilizer matrix has at most one  $X/Y$  literal (if  $X/Y$  literals exist in the column) and one  $Z$  literal (if  $Z$  literals exist in the column), and (ii) remove the rows and columns containing such literals. The resulting stabilizer matrix represents the reduced mixed state.

---

#### Algorithm 5.4 Computation of stabilizer bivectors

---

**Input:** Stabilizer matrices  $\mathcal{M}^\psi$  and  $\mathcal{M}^\phi$  representing  $|\psi\rangle$  and  $|\phi\rangle$ , respectively  
**Output:** Stabilizer matrix  $\mathcal{M}^{\psi \wedge \phi}$  for bivector  $|\psi \wedge \phi\rangle$ , if it exists  
 $\Rightarrow$  BASISNORMCIRC( $\mathcal{M}^\psi$ ) returns circuit  $\mathcal{C}$  such that  $\mathcal{C}|\psi\rangle = |b\rangle$ , where  $|b\rangle$  is a basis state  
 $\Rightarrow$  CONJ( $\mathcal{M}, \mathcal{C}$ ) conjugates  $\mathcal{M}$  by Clifford or Pauli operator  $\mathcal{C}$  and returns the modified matrix  
 $\Rightarrow$  GAUSS( $\mathcal{M}$ ) reduces  $\mathcal{M}$  to canonical form  
 $\Rightarrow$  TENSOR( $\mathcal{M}^\psi, \mathcal{M}^\phi$ ) computes  $|\psi\rangle \otimes |\phi\rangle$  and returns the resulting matrix  $\mathcal{M}^{\psi \otimes \phi}$  (Proposition 3)  
 $\Rightarrow$  INPROD( $\mathcal{M}^\psi, \mathcal{M}^\phi$ ) computes and returns  $\langle \psi | \phi \rangle$   
 $\Rightarrow$  SUM( $\mathcal{M}^{b_1}, \mathcal{M}^{b_2}$ ) computes  $|b_1\rangle - |b_2\rangle$  and returns the resulting matrix  $\mathcal{M}^{b_1 - b_2}$

```

1:  $\alpha \leftarrow \text{INPROD}(\mathcal{M}^\psi, \mathcal{M}^\phi)$  ▷ Apply Algorithm 5.2
2: GAUSS( $\mathcal{M}^\psi$ ) ▷ Set  $\mathcal{M}^\psi$  to canonical form
3: GAUSS( $\mathcal{M}^\phi$ ) ▷ Set  $\mathcal{M}^\phi$  to canonical form
4: if ( $\alpha = 0$  and  $\mathcal{M}^\psi$  dissimilar from  $\mathcal{M}^\phi$ ) or ( $\alpha = 1$ ) or ( $0 < \alpha < 1/\sqrt{2}$ ) then
5:   exit ▷ By Theorem 19
6: end if
7: if  $\mathcal{M}^\psi$  dissimilar from  $\mathcal{M}^\phi$  then ▷ 1-neighbor case from Theorem 19
8:    $\mathcal{M}^\phi \leftarrow \text{CONJ}(\mathcal{M}^\psi, P)$  ▷  $\mathcal{M}^\phi$  now represents  $P|\psi\rangle$ , where  $P$  is a Pauli operator
9: end if
10:  $\mathcal{M}^{\psi \otimes \phi} \leftarrow \text{TENSOR}(\mathcal{M}^\psi, \mathcal{M}^\phi)$ 
11:  $\mathcal{M}^{\phi \otimes \psi} \leftarrow \text{TENSOR}(\mathcal{M}^\phi, \mathcal{M}^\psi)$ 
12:  $\mathcal{C} \leftarrow \text{BASISNORMCIRC}(\mathcal{M}^{\psi \otimes \phi})$  ▷ Obtains basis-normalization circuit
13:  $\mathcal{M}^{b_1} \leftarrow \text{CONJ}(\mathcal{M}^{\psi \otimes \phi}, \mathcal{C})$  ▷ Maps  $\mathcal{M}^{\psi \otimes \phi}$  to basis state  $|b_1\rangle$ 
14:  $\mathcal{M}^{b_2} \leftarrow \text{CONJ}(\mathcal{M}^{\phi \otimes \psi}, \mathcal{C})$  ▷ Maps  $\mathcal{M}^{\phi \otimes \psi}$  to basis state  $|b_2\rangle$ 
15:  $\mathcal{M}^{b_1 - b_2} \leftarrow \text{SUM}(\mathcal{M}^{b_1}, \mathcal{M}^{b_2})$  ▷ Obtains matrix for  $|b_1\rangle - |b_2\rangle$  (proof of Lemma 2)
16:  $\mathcal{M}^{\psi \wedge \phi} \leftarrow \text{CONJ}(\mathcal{M}^{b_1 - b_2}, \mathcal{C}^\dagger)$ 
17: return  $\mathcal{M}^{\psi \wedge \phi}$ 

```

---

## 6 Empirical Studies

Our circuit-synthesis (Section 5.1) and inner-product (Section 5.2) algorithms hold potential to be used in several practical applications including quantum error correction, quantum-circuit simulation, and the computation of geometric measures of entanglement. Therefore, we implemented these algorithms in C++ and empirically validated their performance. Recall that the runtime of Algorithm 5.1 is dominated by the two nested for-loops (lines 20-35). The number of times these loops execute depends on the amount of entanglement in the input stabilizer state. In turn, the number of entangled qubits depends on the the number of CNOT gates in the circuit  $\mathcal{C}$  used to generate the stabilizer state  $\mathcal{C}|0^{\otimes n}\rangle$  (Theorem 7). By a simple heuristic argument [2], one generates highly entangled stabilizer states as long as the number of CNOT gates in  $\mathcal{C}$  is proportional to  $n \log_2 n$ . Therefore, we generated random  $n$ -qubit stabilizer circuits for  $n \in \{20, 40, \dots, 500\}$  as follows: fix a parameter  $\beta > 0$ ; then choose  $\beta \lceil n \log_2 n \rceil$  unitary gates (CNOT, Phase or Hadamard) each with probability  $1/3$ . Then, each random  $\mathcal{C}$  is applied to the  $|00\dots 0\rangle$  basis state to generate random stabilizer matrices (states). The use of randomly generated benchmarks is justified for our experiments because (i) our algorithms are not explicitly sensitive to circuit topology and (ii) random stabilizer circuits are considered representative [25]. Both our inner-product and exterior-product algorithms exhibited similar asymptotic runtime behavior since the bottleneck in both algorithms is the execution of Algorithm 5.1. Therefore, for conciseness, we present experimental results only for our inner-product algorithm. For each  $n$ , we applied Algorithm 5.2 to pairs of random stabilizer matrices and measured the number of seconds needed to compute the inner product. The entire procedure was repeated for increasing degrees of entanglement by ranging  $\beta$  from 0.6 to 1.2 in increments of 0.1. Our results are shown in Figure 8-a. The runtime of Algorithm 5.2 appears to grow quadratically in  $n$  when  $\beta = 0.6$ . However, when we double the number of unitary gates ( $\beta = 1.2$ ), the runtime exhibits cubic growth. Therefore, Figure 8-a shows that the performance of Algorithm 5.2 is highly dependent on the degree of entanglement in the input stabilizer states. Figure 8-b shows the average size of the basis-normalization circuit returned by the calls to Algorithm 5.1. As

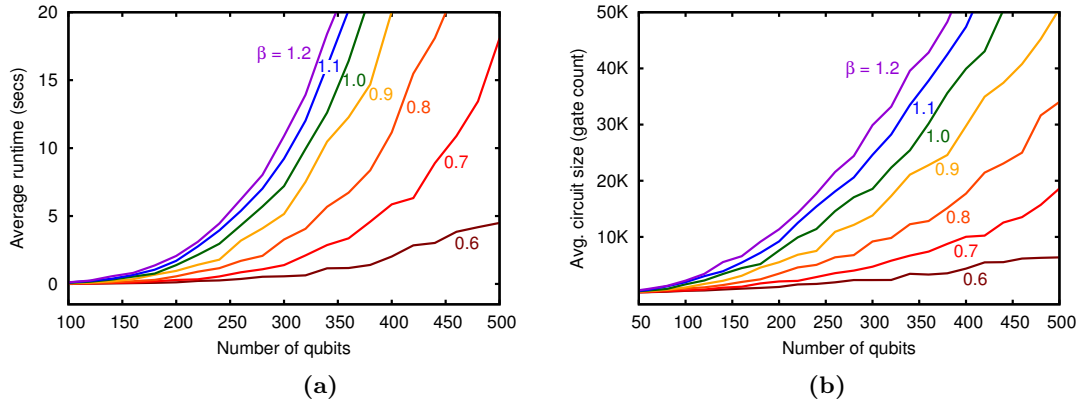


Fig. 8. (a) Average runtime for Algorithm 5.2 to compute the inner product between two random  $n$ -qubit stabilizer states. The stabilizer matrices that represent the input states are generated by applying  $\beta n \log_2 n$  unitary stabilizer gates to  $|0^{\otimes n}\rangle$ . (b) Average number of gates in the circuits produced by Algorithm 5.1.



expected (Proposition 29), the size of the circuit grows quadratically in  $n$ . Figure 9 shows the average runtime for Algorithm 5.2 to compute the inner product between: (i) the all-zeros basis state and random  $n$ -qubit stabilizer states, and (ii) the  $n$ -qubit GHZ state and random stabilizer states. GHZ states are maximally entangled states of the form  $|GHZ\rangle = \frac{|0^{\otimes n}\rangle + |1^{\otimes n}\rangle}{\sqrt{2}}$  that have been realized experimentally using several quantum technologies and are often encountered in practical applications such as error-correcting codes and fault-tolerant architectures. Figure 9 shows that, for such practical instances, Algorithm 5.2 computes the inner product in roughly  $O(n^2)$  time (e.g.,  $\langle GHZ|0\rangle$ ). However, without apriori information about the input stabilizer matrices (e.g., a measure of the amount of the entanglement), one can only say that the performance of Algorithm 5.2 will be somewhere between quadratic and cubic in  $n$ . We compared Algorithm 5.1 to the circuit synthesis approach developed by Audenaert and Plenio (AP) [4] as part of their inner-product algorithm. The benchmark consists of randomly generated  $n$ -qubit stabilizer circuits with  $n \log n$  unitary gates. Figure 10 shows that the AP algorithm produces (non-canonical) circuits with more than twice as many gates as our canonical circuits and takes roughly twice as long to produce them.

## 7 Conclusions

The stabilizer formalism facilitates compact representation of stabilizer states and efficient simulation of stabilizer circuits [2, 16, 17]. Stabilizer states arise in applications of quantum information processing, and their efficient manipulation via geometric and linear-algebraic operations may lead to additional insights in quantum entanglement, quantum error correction and quantum-circuit simulation. Furthermore, stabilizer states are closely related to valence-bond states [35], cluster/graph states [3, 13, 21], and measurement-based/one-way quantum computation [30]. The emphasis of our work on the full set of (pure)  $n$ -qubit stabilizer states is justified by the desire to succinctly represent as many quantum states as possible [1]. This is in contrast to identifying structured representations of more specialized quantum states.

In this work we characterized the nearest-neighbor structure of stabilizer states and quantified the distribution of angles between pairs of stabilizer states. We showed that, for any

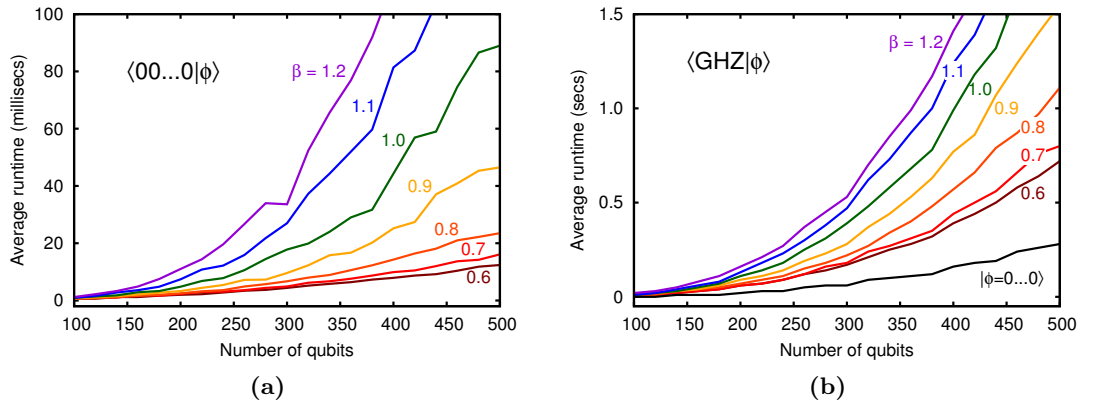


Fig. 9. Average runtime for Algorithm 5.2 to compute the inner product between (a)  $|0^{\otimes n}\rangle$  and random stabilizer state  $|\phi\rangle$  and (b) the  $n$ -qubit GHZ state and random stabilizer state  $|\phi\rangle$ .

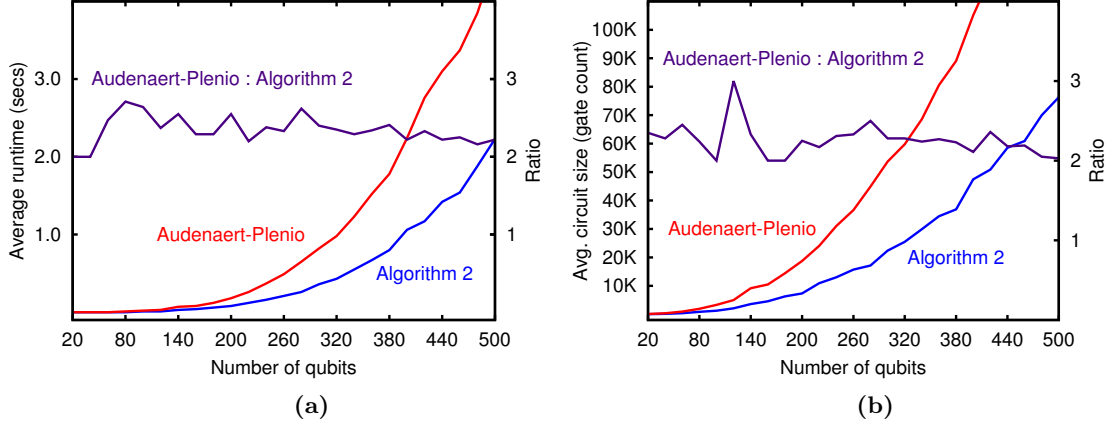


Fig. 10. **(a)** Runtime and **(b)** circuit-size comparisons between Algorithm 5.1 and the circuit synthesis portion of the Audenaert-Plenio inner-product algorithm. On average, Algorithm 5.1 runs roughly twice as fast and produces canonical circuits that contain less than half as many gates. Furthermore, the Audenaert-Plenio circuits are not canonical.

$n$ -qubit stabilizer state  $|\psi\rangle$ , almost all stabilizer states are either orthogonal or nearly orthogonal to  $|\psi\rangle$  as  $n \rightarrow \infty$ . Although the geometric structure of stabilizer states is fairly uniform [11, 24, 26], we showed that local search is not guaranteed to find the closest stabilizer state to an arbitrary quantum state. Furthermore, we defined a family of unbiased states that cannot be approximated by polynomial-sized superpositions of stabilizer states, and proved that the maximal radius of any  $2^n$ -dimensional ball centered at a point on the unit sphere that does not contain any  $n$ -qubit stabilizer states cannot exceed  $\sqrt{2}$ , but approaches  $\sqrt{2}$  as  $n \rightarrow \infty$ . We studied algorithms for: (i) computing the inner product between stabilizer states, (ii) orthogonalizing a set of stabilizer states, and (iii) computing stabilizer bivectors. A crucial step of our inner-product algorithm is the synthesis of a circuit that transforms a stabilizer state into a computational-basis state. Our algorithm synthesizes such circuits using a 5-block canonical template structure using  $O(n^2)$  stabilizer gates. Our technique produces circuits with half as many gates as the approach from [4] using a block sequence that is shorter than the approach from [2]. We analyzed the performance of our inner-product algorithm and showed that, although its runtime is  $O(n^3)$ , it can take quadratic time in practice.

**Open problems.** As reviewed in Section 5, the work in [2, 4, 31] describes how to represent and manipulate mixed states using the stabilizer formalism. To this end, extensions of our results to mixed states could be of interest. Several approaches have been proposed for generalizing the stabilizer representation to represent arbitrary quantum states and simulate non-stabilizer circuits [2, 32]. An open question is whether the geometric properties of stabilizer states shown in this work can be exploited to improve simulation of generic quantum circuits while ensuring the scalability of simulation when stabilizer gates dominate. Another attractive direction for future work is generalizing presented results and algorithms to the case of  $d$ -dimensional qudit states [9]. Further challenges include:

- Characterization of possible volumes of high-dimensional parallelotopes formed by more than two stabilizer vectors (generalizing Proposition 20).

- Characterization of minimally-dependent sets of stabilizer states and algorithms for efficient detection of such sets (extending our discussion in Section 3.3).
- Efficiency improvement for computing inner and exterior products of stabilizer states as well as the orthogonalization procedure from Algorithm 5.3.
- Characterization of the complexity analysis of finding a closest stabilizer state to a given non-stabilizer state (for appropriate representations of non-stabilizer states).
- Describing the Voronoi-diagram structure of stabilizer states (extending Theorem 13).

**Acknowledgements.** The authors would like to thank the Microsoft Research QuArC group for questions and suggestions, Dmitri Maslov for inspiring discussions, and anonymous reviewers for suggested improvements. This work was sponsored in part by the Air Force Research Laboratory under agreement FA8750-11-2-0043.

## References

1. S. Aaronson, “Multilinear formulas and skepticism of quantum computing,” Proc. STOC ’04, pp. 118–127 (2004).
2. S. Aaronson and D. Gottesman, “Improved simulation of stabilizer circuits,” Phys. Rev. A, vol. 70, no. 052328 (2004).
3. S. Anders and H. J. Briegel, “Fast simulation of stabilizer circuits using a graph-state representation,” Phys. Rev. A, vol. 73, no. 022334 (2006).
4. K. M. R. Audenaert and M. B. Plenio, “Entanglement on mixed stabiliser states: normal forms and reduction procedures,” New J. Phys., vol. 7, no. 170 (2005).
5. A. Calderbank, E. Rains, P. Shor, and N. Sloane, “Quantum error correction via codes over  $GF(4)$ ,” IEEE Trans. Inf. Theory, vol. 44, pp. 1369–1387 (1998).
6. R. Cleve and D. Gottesman, “Efficient computations of encodings for quantum error correction,” Phys. Rev. A, vol. 56, pp. 1201–1204 (1997).
7. O. Dahlsten and M. B. Plenio, “Exact entanglement probability distribution of bi-partite randomised stabilizer states,” Quant. Inf. Comp., vol. 6, no. 527 (2006).
8. A. Datta and G. Vidal, “Role of entanglement and correlations in mixed-state quantum computation,” Phys. Rev. A, vol. 75, no. 042310 (2007).
9. N. de Beaudrap, “A linearized stabilizer formalism for systems of finite dimension,” Quant. Inf. Comp., vol. 13, pp. 73–115 (2013).
10. J. Dehaene and B. De Moor, “Clifford group, stabilizer states, and linear and quadratic operations over  $GF(2)$ ,” Phys. Rev. A, vol. 68, no. 042318 (2003).
11. D. P. DiVincenzo, D. W. Leung and B. M. Terhal, “Quantum data hiding,” IEEE Trans. Inf. Theory, vol. 48, no. 3, pp. 580–599 (2002).
12. I. Djordjevic, “Quantum information processing and quantum error correction: an engineering approach,” Academic press (2012).
13. W. Dur, H. Aschauer and H.J. Briegel, “Multiparticle entanglement purification for graph states,” Phys. Rev. Lett., vol. 91, no. 107903 (2003).
14. C. Emary, “A bipartite class of entanglement monotones for  $N$ -qubit pure states,” J. Phys. A: Math. Gen., vol. 37, no. 8293 (2004).
15. D. Fattal, T. S. Cubitt, Y. Yamamoto, S. Bravyi and I. L. Chuang, “Entanglement in the stabilizer formalism,” arxiv:0406168 (2004).
16. D. Gottesman, “Stabilizer codes and quantum error correction,” Caltech Ph.D. thesis (1997).
17. D. Gottesman, “The Heisenberg representation of quantum computers,” arXiv:9807006v1 (1998).
18. O. Guehne, G. Toth, P. Hyllus and H.J. Briegel, “Bell inequalities for graph states,” Phys. Rev. Lett. 95, 120405 (2005).
19. A. W. Harrow and R. A. Low, “Random quantum circuits are approximate 2-designs,” Comm. Math. Phys., vol. 291, no. 1, pp. 257–302 (2009).

20. M. Hayashi, et al., “Entanglement of multiparty stabilizer, symmetric, and antisymmetric states,” *Phys. Rev. A*, vol. 77, no. 012104 (2008).
21. M. Hein, J. Eisert, and H.J. Briegel, “Multi-party entanglement in graph states,” *Phys. Rev. A*, vol. 69, no. 062311 (2004).
22. H. Heydari, “Quantum entanglement measure based on wedge product,” *Quant. Inf. Comp.*, vol. 6, pp. 166–172 (2006).
23. R. Jozsa, “Embedding classical into quantum computation,” arXiv:0812.4511 (2008).
24. A. Klappenecker and M. Roetteler, “Mutually unbiased bases are complex projective 2-designs,” arXiv:0502031 (2005).
25. E. Knill, et al., “Randomized benchmarking of quantum gates,” *Phys. Rev. A*, vol. 77, no. 1 (2007).
26. A. Montanaro, “On the distinguishability of random quantum states,” *Comm. in Math. Phys.*, vol. 273, no. 3, pp. 619–636 (2007).
27. C. Moore and M. Nilsson, “Parallel quantum computation and quantum codes,” *SIAM Journal on Comp.*, vol. 31, no. 3, pp. 799–815 (2001).
28. M. A. Nielsen and I. L. Chuang, “Quantum Computation and Quantum Information,” (Cambridge University Press, 2000).
29. K. N. Patel, I. L. Markov and J. P. Hayes, “Optimal synthesis of linear reversible circuits,” *Quant. Inf. Comp.*, vol. 8, no. 3 (2008).
30. R. Raussendorf, D. E. Browne and H. J. Briegel, “Measurement-based quantum computation on cluster states,” *Phys. Rev. A*, vol. 68, no. 022312 (2003).
31. G. Smith and D. Leung, “Typical entanglement of stabilizer states,” *Phys. Rev. A*, vol. 74, no. 062314 (2006).
32. M. Van den Nest, “Classical simulation of quantum computation, the Gottesman-Knill theorem, and slightly beyond,” *Quant. Inf. Comp.*, vol. 10, pp. 0258–0271 (2010).
33. M. Van den Nest, J. Dehaene and B. De Moor, “On local unitary versus local Clifford equivalence of stabilizer states,” *Phys. Rev. A*, vol. 71, no. 062323 (2005).
34. F. Verstraete, J. I. Cirac and J. I. Latorre, “Quantum circuits for strongly correlated quantum systems,” *Phys. Rev. A*, vol. 79, no. 032316 (2009).
35. F. Verstraete and J. I. Cirac, “Valence-bond states for quantum computation,” *Phys. Rev. A*, vol. 70, no. 060302 (2004).
36. T.-C. Wei and P. M. Goldbart, “Geometric measure of entanglement and applications to bipartite and multipartite quantum states,” *Phys. Rev. A*, vol. 68, no. 042307 (2003).
37. H. Wunderlich and M. B. Plenio, “Quantitative verification of fidelities and entanglement from incomplete measurement data,” *J. Mod. Opt.*, vol. 56, pp. 2100–2105 (2009).

## Appendix A

### The 1080 three-qubit stabilizer states

Shorthand notation represents a stabilizer state as  $\alpha_0, \alpha_1, \alpha_2, \alpha_3$  where  $\alpha_i$  are the normalized amplitudes of the basis states. Basis states are emphasized in bold. The  $\angle$  column indicates the angle between that state and  $|000\rangle$ , which has 28 1-neighbor states and 315 orthogonal states ( $\perp$ ). The tables are intended for on-screen viewing under magnification.

[illegible]

